國立臺灣大學生物資源暨農學院園藝暨景觀學系

碩士論文

Department of Horticulture and Landscape Architecture
College of Bioresources and Agriculture
National Taiwan University

Master thesis

酪梨後熟期間果實密度及性狀特徵之研究

A Study of the Correlation Between Fruit Density and Physical Properties on Avocado Ripening

久住あかね

Akane KUSUMI

指導教授：林書妍 博士

Advisor: Shu-Yen Lin, Ph.D.

中華民國 112 年 7 月

July, 2023

doi:10.6342/NTU202302656

Abstract

Avocado (*Persea americana*) is a globally traded fruit, and its condition during harvest can affect the successful ripening and time required to reach the optimal edible state. Although numerous harvesting guidelines exist, non-destructive techniques for predicting the ripening period are insufficient. This study aimed to establish a non-destructive density measurement by the 3D reconstruction method as an indicator for avocado ripening prediction. Fruits of 'Red Fairy', 'Choquette', and 'Hass' were measured for weight, volume, firmness, and skin color every 2 days during ripening. Besides, 3D models of fruits were acquired every 2 days, too, and seed characteristics were evaluated at ripening. When the firmness of a fruit measured by a texture analyzer reached below 10N, it was regarded as ripe. The fruits were divided into 3 groups based on the first density measurement. When the earliest fruits reached ripening, the highest density groups of 'Red Fairy' and 'Hass' showed significantly higher firmness and greener color, indicating slower ripening; that of 'Choquette' exhibited significantly lower firmness and bigger color change, indicating faster ripening. Although the opposite trend was observed, it roughly succeeded to classify slow- or fast-ripening fruit by density. Then, regression models were developed since significant correlations were observed between whole fruit density and firmness or color indicators from different days. However, their R-squared values were less than 0.50, implying that those models may not be suitable for predicting those parameters practically. Further consideration of seed size or seed space did not improve correlation coefficients and R-squared values. Finally, an investigation was conducted with 'Red Fairy' to determine whether the 3D reconstruction method could replace the displacement method, which has been conventionally used in measuring the fruit volume. Volume measurements using two different methods showed a significant similarity ($R^2 = 0.988$, $p < 0.01$), highlighting the efficiency of the 3D

doi:10.6342/NTU202302656

reconstruction method. Density classifications based on the reconstruction method also demonstrated that the highest-density group tended to ripen slowly, matching the results obtained by the displacement method. Those results demonstrate that simple fruit characteristic measurements can provide a preliminary estimation of avocado ripening behavior.

Keywords: *Persea americana*, ripeness, density, volume estimation, 3D imaging

doi:10.6342/NTU202302656

中文摘要

酪梨（*Persea americana*）是一種全球貿易的水果，果實收穫時的狀態會影響後熟與否和達到最佳食用狀態所需的時間。 儘管關於酪梨採收的判斷已有許多採收指標，但用於預測後熟期的非破壞性技術仍然不足。本研究旨在建立一種非破壞性的密度測量方法，以三維重建法作為預測酪梨後熟的指標，並了解‘Red Fairy’、‘Choquette’和‘Hass’三個品種酪梨在後熟期間的物性變化。自果實採收後開始，在果實後熟期間每 2 天進行重量、體積、硬度和果皮顏色的測量。此外，每 2 天拍攝果實的三維模型，並在成熟時評估種子特性。當質構儀測得的水果硬度達到 10N 以下時，即視為完全後熟。根據果實第一次密度測量的結果將其分為高、中、低共 3 組密度。當有果實開始達到後熟時，‘Red Fairy’和‘Hass’的最高密度組顯示出較高的硬度和較綠的顏色，表明成熟較慢；‘Choquette’的最高密度組顯示出顯著較低的硬度和較大的顏色變化，表明成熟較快。由於整個水果密度與不同天數的硬度或顏色指標之間存在顯著相關性，因此建立了回歸模型。然而，模型的 R 平方值小於 0.50，說明在建構的模型尚無法很好的預測，所使用的參數可能需要更多考量，雖然進一步考慮種子大小或種子空間，但並未改善相關係數和 R 平方值。最後，以 ‘Red Fairy’為材料，確定應用三維重建法是否可以取代傳統用於測量水果體積的排水法。使用兩種不同方法進行的體積測量具有顯著的相關性（$R2 = 0.988$，$p < 0.01$），說明使用三維重建法可以替代傳統排水法，而三維拍攝重建法量測體積具有好的效率。基於重建法的密度分類也表明最高密度組傾向於成熟緩慢，這與排水法獲得的結果相符。總和以上結果，對採收後、剛開始後熟的果實，以簡單的果實物理特性測量結果可以提供酪梨後熟行為的初步預估。

關鍵字：酪梨、後熟、密度、體積測量、三維影像

doi:10.6342/NTU202302656

Table of Contents

Introduction 1

Avocado fruit maturity 2

Avocado ripening and issues 3

Predicting avocado fruit ripening status 4

The relationship between fruit maturity at harvest and post-harvest ripening 5

Density at the beginning of ripening as a parameter of fruit quality 6

Density changes during ripening in avocado fruits 8

Fruit volume measurement method 8

Objectives 10

Materials and Methods

Avocado samples and storage conditions 11

Acquirement of ripening parameters during ripening 11

Acquirement of other parameters during ripening 12

Development of fruit models with the 3D reconstruction method 12

Parameters measured after fruit reached ripening 13

Statistical analysis 14

Results and Discussions

Determination of the definition of ripening 15

Ripening traits of each sample batch of three tested avocado cultivars 16

Changes in measured parameters during ripening 16

doi:10.6342/NTU202302656

Results of principal component analysis showing factors that contributed to the ripening 18
Relationships between density and firmness or color 20
Predictions of ripening parameters based on whole fruit density calculated by the displacement method 21
Effect of seed weight and seed space on whole fruit density 23
Potential factors weakening relationships between density and ripening 25
Comparison of relations of whole fruit density and firmness during ripening with respect to firmness 26
Comparison of volume measurement by the displacement method and the 3D reconstruction method 28
The relationship between ripening speed and fruit classification based on density measured by the 3D reconstruction method 28
Predictions of ripening parameters based on whole fruit density calculated by the 3D reconstruction method 29
Conclusions 31

References 33

doi:10.6342/NTU202302656

List of Tables

Table 1. Summary of avocado samples and storage conditions in the present study. 43

Table 2. Ripening traits of each sample batch of three tested avocado cultivars..... 44

Table 3. Time required for ripening and number of fruits in the three cultivars..... 45

Table 4. Density ranges of low-density, medium-density, and high-density groups.. 46

Table 5. Spearman's rank correlation coefficients between density and firmness from different days of ripening in 'Red Fairy' 47

Table 6. Spearman's rank correlation coefficients between density and firmness from different days of ripening in 'Choquette'..... 48

Table 7. Spearman's rank correlation coefficients between density and firmness from different days of ripening in 'Hass' 49

Table 8. Spearman's rank correlation coefficients between density and a* value of color value from different days of ripening in 'Red Fairy'..... 50

Table 9. Spearman's rank correlation coefficients between density and b* value of color value from different days of ripening in 'Choquette' 51

Table 10. Spearman's rank correlation coefficients between density and a* value of color value from different days of ripening in 'Hass'..... 52

Table 11. The best regression models for firmness prediction with the highest R-squared 53

Table 12. The best regression models for color prediction with the highest R-squared 54

Table 13. Correlation coefficients between whole fruit density, seed size, and seed space at ripening 55

Table 14. Spearman's rank correlation coefficients between density subtracting seed size (DS) and firmness from different days of ripening in 'Red Fairy'..... 56

doi:10.6342/NTU202302656

Table 15. Spearman's rank correlation coefficients between density subtracting seed size (DS) and firmness from different days of ripening in 'Choquette' 57
Table 16. Spearman's rank correlation coefficients between density subtracting seed size (DS) and firmness from different days of ripening in 'Hass' 58
Table 17. The best regression models to predict firmness based on density subtracting seed size (DS) for each cultivar 59
Table 18. Spearman's rank correlation coefficients between density subtracting seed size and space (DC) and firmness from different days of ripening in 'Red Fairy' 60
Table 19. Spearman's rank correlation coefficients between density subtracting seed size and space (DC) and firmness from different days of ripening in 'Choquette' 61
Table 20. Spearman's rank correlation coefficients between density subtracting seed size and space (DC) and firmness from different days of ripening in 'Hass' 62
Table 21. Spearman's rank correlation coefficients between firmness and firmness from different days of ripening in 'Red Fairy' 63
Table 22. Spearman's rank correlation coefficients between firmness and firmness from different days of ripening in 'Choquette' 64
Table 23. Spearman's rank correlation coefficients between firmness and firmness from different days of ripening in 'Hass' 65
Table 24. Spearman's rank correlation coefficients between whole fruit density measured by the 3D reconstruction method and firmness from different days of ripening in 'Red Fairy' 66

doi:10.6342/NTU202302656

Table 25. Spearman's rank correlation coefficients between whole fruit density measured by the 3D reconstruction method and a* value from different days of ripening in 'Red Fairy' 67

doi:10.6342/NTU202302656

List of Figures

Fig. 1. Hypothesized relationships among maturity, ripening, and density 68

Fig. 2. Two different ways to measure fruit volume 69

Fig. 3. Example of the acquisition of a 3D model of an avocado fruit 70

Fig. 4. Examples of developed 3D models 71

Fig. 5. The definitions of seed cavity and seed space in this study..... 72

Fig. 6. Firmness changes in 'Red Fairy' batch 1 during ripening shown with boxplots 73

Fig. 7. Weight changes during ripening 74

Fig. 8. Volume changes measured by the displacement method during ripening 75

Fig. 9. Differences in peel color from Day 1 to ripening..... 76

Fig. 10. Changes in color parameters during ripening of 'Red Fairy' fruit 77

Fig. 11. Changes in color parameters during ripening of 'Choquette' fruit 78

Fig. 12. Changes in color parameters during ripening of 'Hass' fruit..... 79

Fig. 13. Firmness changes during ripening 80

Fig. 14. Density changes during ripening 81

Fig. 15. Heatmap showing density change in the individual fruit during ripening.... 82

Fig. 16. The plots of principal component analysis showing strength of relevance of each parameter to ripening..... 83

Fig. 17. Density range of 'Hass' fruits on Day 1 85

Fig. 18. Relationships between density and firmness or color value from all measurements..... 86

Fig. 19. Distribution of density among different density groups 87

Fig. 20. Boxplots showing firmness and color differences among density groups ... 88

doi:10.6342/NTU202302656

Fig. 21. Relationships between whole fruit density and firmness where the maximum R-squared was observed in the regression analysis 89
Fig. 22. Relationships between whole fruit density and color values where the maximum R-squared was observed in the regression analysis 90
Fig. 23. Cross sections of avocado fruit and the magnitude of seed space in fruit 91
Fig. 24. Scatter plots showing the relationships between seed size or seed space, and fruit size 92
Fig. 25. Relationships between density subtracting seed size (DS) and firmness where the maximum R-squared was observed in the regression analysis 93
Fig. 26. Summary of the relationships among maturity, ripening, and density found in this study 94
Fig. 27. Relationships between dry matter (DM) content and density subtracting seed size and space (DC) at ripening 95
Fig. 28. A plot of the volume of 'Red Fairy' fruits measured by the displacement method and volume measured by the 3D reconstruction method 96
Fig. 29. Plots of the fruit width and fruit length of 'Red Fairy' fruits measured by the displacement method and volume measured by the 3D reconstruction method 97
Fig. 30. Boxplots showing density, firmness, and color differences among density groups based on the 3D reconstruction method 98

doi:10.6342/NTU202302656

Introduction

Avocado (*Persea americana*) is a tropical or semi-tropical fruit that has recently been attracting much attention due to its richness in unsaturated fatty acids (Hernández et al., 2016). Avocado can be divided into three races based on origins, Mexican, Guatemalan, and West Indian (Storey et al., 1986; Bergh and Ellstrand, 1986). Though 'Hass' is the leading cultivar around the world, its cultivation in Taiwan is not easy due to the unsuitable climate (Wu et al., 2007). Cultivars planted there include local cultivars such as 'Black Beauty' or 'Red Fairy' and foreign cultivars such as 'Hall' or 'Choquette' (Wu et al., 2023). However, because most research has been done on 'Hass', ripening patterns have not been well reported in cultivars grown in Taiwan.

Avocado is a typical climacteric fruit (Sacher, 1962), and its ripening pattern will highly affect storage control during the long way transportation. Japan is the main avocado importer in Asia. In 2022, approximately 50,573 tons of avocado were imported, with 75% of them 'Hass' from Mexico (MAFF, 2023). Fruits are harvested at a relatively young stage so that they will be tolerant to long ship journeys to Japan under cold storage conditions. Once the fruits arrive, they are put into warehouses designed for storage and triggering ripening (Yokohama Customs, 2021). Since the ripening patterns can differ among fruits, ripeness is checked by color and sorted for additional ripening treatment or shipping (Funasho Shoji Co., Ltd., n.d.). Developing an effective classification method for harvested fruits, along with an easy manipulation process, would be beneficial to the avocado industry. This would not only improve the quality for importers but also provide exporters with a means to control fruit ripening.

doi:10.6342/NTU202302656

Avocado fruit maturity

Avocado has a unique ripening characteristic as a climacteric fruit. It matures but never ripens while attached to the tree, thus determination of maturity is extremely important since it affects post-harvest ripening and fruit quality. The horticultural maturity of avocado fruit can be generally defined as the point of fruit growth at which fruit can ripen normally without any shriveling and can become suitable for eating after the fruit is detached from the tree (Flitsanov et al., 2000). The most widely applied indicator for maturity determination is oil content and dry matter (DM) (Hofman et al., 2002). Avocado fruit mesocarp starts to accumulate oil a few weeks after the fruit set (Ozdemir and Topuz, 2004). Those oils are mainly composed of oleic acid (C18:1) and palmitic acid (C16:0) (Teng et al., 2016), and their buildup lasts through development (Shezi et al., 2020). Therefore, higher oil content represents higher maturity. However, the measurement of oil content is complex and costs a lot requiring chemical-based extractions, thus alternatives were explored which could be suitable on the commercial scale (Ncama et al., 2018; Lewis et al., 1978). DM content has been proven to be closely related to oil content (Lee et al., 1983). Besides, since DM and water content are complementary to each other, water content % is also used. In terms of exports, to assure normal ripening and fruit quality, several countries have settled the minimum DM content for harvest in each cultivar (Hofman et al., 2002). Conventionally, DM has been obtained by dividing the weight of fresh pulp by the weight of dried pulp when the pulp is dried to remove water and the weight does not change anymore (Woolf et al., 2003). Non-invasive techniques to predict DM have also been proposed with NIR being the most promising method (Wedding et al., 2012). NIR spectra provide information on the oil-specific chemical bonds, and the DM content can be inferred from its absorption or reflectance ratio (Schmilovitch et al., 1997; Clark et al., 2003).

doi:10.6342/NTU202302656

Avocado ripening and issues

Avocado ripening is accompanied by dramatic increases in endogenous ethylene production and respiration (Bennett et al., 1987; Feng et al., 2000). Additionally, several physiological changes occur within a fruit during ripening. Due to respiration, consuming the sugars and water inside the fruit, emitting vapor and carbon dioxide outside, mass loss increases (Arzate-Vázquez et al., 2011). Besides, firmness also changes. It decreases gradually at the beginning of the ripening, but after the climacteric peak, it drops considerably, followed by a slight change at ripening (Mishra et al., 2021). In addition, the fruit peel color can change obviously in some cultivars. It changes from green to purple or black in 'Hass' (Lin et al., 2020), and 'Maluma' (Ernst, 2011). On the other hand, the peel color remains green with slight changes in other cultivars, such as 'Fuerte' (Osondu et al., 2022; Ahmed et al., 2010) and 'Choquette' (Wang et al., 2010).

One of the biggest issues regarding avocado fruit is its heterogeneity in ripening (Fuentealba et al., 2017). The avocado flowering period can range from 2 to 3 months, resulting in a huge diversity in maturity within the same tree (Lewis, 1978). Besides, it has a climacteric characteristic as mentioned above. It matures but never ripens while attached to the tree, due to the "tree factors". Liu et al. (2002) attributed this to C_7 carbons such as mannoheptulose and perseitol, which can act as inhibitors of ripening. They demonstrated that the main translocating sugar in avocado is C_7 sugars, and the fruit started to ripen even on the tree by inhibiting the sugar transportation by girdling. Thus, fruit ripening occurs rapidly only after being detached from the tree. Due to those factors, avocado shelf life could be short and varied within a batch. This can cause losses from corruption, e.g., rottenness or overripening.

doi:10.6342/NTU202302656

Predicting avocado fruit ripening status

In order to overcome this issue, the prediction of ripening stages is quite important. Melado-Herreros et al. (2021) stated that it is important to optimize the supply chain so that stakeholders can get avocado fruit with the expected quality. Besides, the importance of non-destructive techniques should be emphasized to allow successive measurements through that chain (Zhang et al., 2022). In addition to parameters that are obvious during ripening, such as changes in color and firmness as described above, many models have been proposed to predict the current ripening status based on the relationship with physiological factors.

Some researchers found a clear relationship between ultrasonic signals and fruit firmness. The concept is that the decrease in speed or the reduction in acoustic signals represents the physiochemical or physical change of the sample since the acoustic wave interacts with the molecules inside (Miraei Ashtiani et al., 2016; Awad et al., 2012). Mizrach and Flitsanov (1999) utilized the transducer alignment systems and found a strong correlation between the acoustic signal's attenuation and the avocado fruits' firmness ($R^2 = 0.984$). Since this method required the holding of a transducer and receiver, which can be complex, Gaete-Garretón et al. (2005) invented a new set-up utilizing a single source configuration. The acoustic absorption coefficients and firmness were found to be closely related ($R^2 = 0.976$). Although the acoustic techniques exhibited a high possibility to predict firmness, they concluded that there should be more room for discussing easier and simpler equipment.

Others utilized image processing to detect color change. Cho et al. (2020) focused on the fact that the ripening accompanies a decrease in firmness and color change in 'Hass', developing machine-learning models to predict firmness based on the color of avocado fruit in the photos taken with a smartphone. The best model was obtained by the

doi:10.6342/NTU202302656

support vector regression model with an R-squared of 0.92 and RMSE of 7.54. While this study proposed a very easy and simple system, this may lack versatility, since there are many cultivars with peel color staying green with small changes during ripening, such as 'Ettinger' and 'Pinkerton' (Hershkovitz et al., 2005). It should be confirmed if these kinds of methods could also be applied to green-peel cultivars.

In addition, near-infrared (NIR) spectroscopy or hyperspectral data has been described as promising. Visible light wavelength ranges from approximately 350-780 nm, and NIR wavelength ranges from approximately 780-2500 nm (Wang et al., 2022). The concept is that the reflectance or absorption bands of wavelength is well related to the concentration of specific components inside the fruit (Lorente et al., 2012). Although the NIR spectroscopy captures data within a certain area, the hyperspectral camera can obtain information from all fields of view that the camera lens can capture. Thus, it results in producing a data cube, which has three-dimensional data, the x and y axes of the image, and the z-axis as the different wavelengths (Sowmya et al., 2019). Mishra et al. (2021) developed the firmness prediction model utilizing the full range of Vis-NIR wavelength (350-2500 nm), acquiring the R-squared of 0.87. Maftoonazad et al. (2011) combined the hyperspectral technique with machine learning to extract the relevant wavelength easily. They succeeded to develop models predicting many ripening parameters, including respiration rate, firmness, total color difference, and weight loss. The maximum R-squared and error rate fro firmness prediction was 0.953 and 0.0608, respectively. Although those techniques were described as the most advanced in terms of installation (Magwaza and Tesfay, 2015), there are some drawbacks. Firstly, they represent the information from a certain area of fruits, though different positions could have different ripening statuses. Woolf et al. (1999) revealed that the sun-exposed side and shaded side of one fruit could have different physiological statuses, including firmness and dry weight.

doi:10.6342/NTU202302656

Thus, by applying the method which could represent the whole fruit condition, possibly the prediction can get much closer to the actual status of a fruit. Besides, the vulnerability to errors also should be noted. Those devices are usually highly fine-tuned by calibration, thus quite sensitive to environmental factors like light or temperature. A high level of expertise to operate them is required, too (McGlone et al., 2002). Collectively, a simpler and more direct prediction method could be further explored.

The relationship between fruit maturity at harvest and post-harvest ripening

The relationship between maturity levels and ripening patterns has been examined in avocado fruit. It has been demonstrated that avocado fruit harvested in the later season with high maturity tended to ripen faster, but the one harvested in the earlier season with low maturity took more time to ripen (Blakey et al., 2009; Cutting et al., 1992). Pesis et al. (1978) demonstrated that an increase in cellulase activity and the bigger effects of ethylene on its activity and respiration rate were observed in mature fruit, than in younger fruit. However, this relationship could be affected by the harvest time or locations (Hofman et al., 2000; Rowell, 1988). Since the increase in DM and maturity is connected, some researchers tried to find the relationship between DM and ripening. Although Pedreschi et al. (2014) did not find a clear relationship between them or significant differences in days to ripen among different DM classes, Burdon et al. (2015) discovered a clear relationship ($r = -0.99$) by splitting the DM% into 4% bands. Besides, Blakey et al. (2009) demonstrated that variability in ripening durations was suppressed by immersing the fruits in water, which accelerated the water intake depending on the water potential of each fruit and contributed to the homogenization of DM content among fruit. Therefore, it was suggested that there could be a trend that fruit with lower DM% ripens faster.

doi:10.6342/NTU202302656

Density at the beginning of ripening as a parameter of fruit quality

Density at the beginning of ripening has been utilized as a good parameter to estimate fruit quality in many kinds of fruits. Jordan et al. (2000) demonstrated that kiwifruit (*Actinidia deliciosa*) density at harvest had a high correlation with soluble solid contents at the ripening stage with an R-squared as high as 85.1%. Fruits with high density tended to have higher soluble solid contents. In addition, fruits with high density also exhibited higher DM content with an R-squared of 82.6%. Similar trends have been observed in mango (*Mangifera indica*) and nectarine (*Prunus persica*) (Hor et al., 2020; Aubert et al., 2019). Fruits were considered to accumulate more sugars with the time attached to the trees, since fruits function as a strong sink. Besides that, it was also evidenced that there were relationships between firmness and density. Aubert et al. (2019) reported firmness became significantly lower after ripening in a higher-density class of nectarine fruits at harvest. Hor et al. (2020) also observed that mango fruit with high density had lower firmness after the ripening, followed by the establishment of a regression formula to predict firmness based on density before ripening. They attributed this to the higher maturity of fruits while accumulating photosynthates for a longer period of time on the tree, which accelerated ripening. Therefore, there would be a possibility that fruit density at harvest or before ripening can be an indicator of firmness, which is widely accepted as a ripening parameter. Besides, since avocado maturity at harvest should affect the ripening speed as mentioned above, this relationship between density and ripening pattern may also be found in avocado fruit. The flesh oil of avocado fruit has been reported to have a specific gravity of approximately 0.927 g/cm^3 (Bora et al., 2001). Therefore, theoretically, it may be assumed that fruit with high oil content has low density (Fig. 1). As density measurement requires simpler operation and does not require

doi:10.6342/NTU202302656

high fine-tuning, density could potentially be an alternative to predict the ripening duration (McGlone et al., 2002).

Density changes during ripening in avocado fruits

Besides the diversity of density at harvest, density can also change during ripening. Self et al. (1994) reported that the density of 'Fuerte' avocado fruit increased from 0.963 g/cm^3 on day 1 to 0.979 g/cm^3 on day 15 of storage, although the transition between this duration fluctuated with increases and decreases. Clark et al. (2007) also found that the density of whole fruit, seed, and flesh significantly increased from harvest to ripe. However, they did not explore if the density change during ripening could be utilized to estimate ripening conditions or not, still leaving the space to investigate it in this research (Fig. 1).

Fruit volume measurement method

Conventionally, the water displacement method has been often applied to measure fruit volume with its simplicity (Mohsenin, 1970; Jarimopas et al., 2005). In this method, fruit is sunk into the water and the volume of water replaced is recorded as the volume of the fruit. However, this method could contain several disadvantages. Firstly, it is time-consuming, because the effect of water surface swaying should be minimized to measure the volume precisely (Wang and Li, 2014; Bozokalfa and Kilic, 2010). Besides, this also leads to a high proneness to errors, depending on observers. Moreover, as fruit is put into the water, moisture on the fruit surface should be completely wiped out, otherwise, it produces a favorable environment for fungi to grow. Thus, it requires extra care and carries a risk of being damaged (Koc, 2007). Therefore, non-destructive, quick, and precise volume estimations have been demanded. Those included an optical ring

doi:10.6342/NTU202302656

sensor system (Gall, 1997), a computed tomography system (Maisl et al., 2006), magnetic resonance imaging (Andaur et al., 2004), and more. Among those different techniques, currently, the 2D machine-vision system is applied most widely, with its relatively low cost for the camera and the advantage that the detected fruit color or the external damage could also be used as sorting parameters (Moreda et al., 2009). However, as information on the object depth has been stated to increase the prediction accuracy a lot (Chen et al., 1989; Lee et al., 2001), the 3D scanning method has attracted attention as a promising alternative, although its application on avocado fruit volume measurement has not been reported yet.

doi:10.6342/NTU202302656

Objectives

Few studies have explored density changes during avocado ripening. Besides, the relationship between density and ripening patterns has not been deciphered. Thus, this study aims to cultivate knowledge of the postharvest physiology of avocado fruits and to see the possibility of employing density as a ripening parameter. Furthermore, it was also investigated if the 3D reconstruction method could replace the conventional volume measurement methods, water displacement, and achieve fruit sorting based on density practically.

doi:10.6342/NTU202302656

Materials and Methods

Avocado samples and storage conditions

Three cultivars, ‘Red Fairy’, ‘Choquette’, and ‘Hass’ were used in this study. Their harvest dates, origins, numbers, and storage conditions including temperature and relative humidity are listed in Table 1. Several orchards were chosen to increase the diversity of fruit conditions. Samples were harvested when they were considered to be mature mainly based on their sizes (Day 0) and arrived at the laboratory the next day (Day 1). A batch includes all fruits harvested on the same day. It should be noted that the ‘Choquette’ fruits of batch 3 from Taichung arrived at the laboratory on Day 2, due to shipping issues, thus lacking any measurements on Day 1.

Acquirement of ripening parameters during ripening

Avocado firmness (N) was non-destructively measured every 2 days since Day 1 with TA.XTPlus texture analyzer (Stable Micro System, Surrey, England). For each measurement, a cylinder probe (8 mm in diameter) pressed two points at the equational region at a depth of 1.5mm for ‘Red Fairly’ and ‘Choquette’, and three points for ‘Hass’. The different numbers of pushing points in ‘Hass’ was to overcome the value variability caused by the rough skin of the fruit. The trigger force was set to 0.049N and the maximum force recorded during the measurement was used as the fruit firmness. Fruit skin color was measured in triplicate on every three parts, calyx, equational, and apex region with a Minolta Chroma Meter CR 400 (Konica Minolta, Osaka, Japan), producing L* (lightness), a*, b*, C* (chroma) and h° (hue angle) value. They are based on L*a*b* color space and L*C*h color space. Higher L* represents whiter color, a* represents the intensity of red/green (-a = green; +a = red), and b* represents the intensity of blue/yellow (-b = blue; +b = yellow) (Mardigan et al., 2014; Khajehdizaj et al., 2014). Besides, a

doi:10.6342/NTU202302656

higher C* represents more vivid color, and h° represents the angle between a* value and b* value, with being calculated by the following formulas, respectively (Xi et al., 2021);

$$C^* = \sqrt{a^{*2} + b^{*2}}$$

$$h° = \tan^{-1}\left(\frac{b^*}{a^*}\right)$$

Acquirement of other parameters during ripening

Fruit weight (g) was measured every day by an electronic scale. Fruit volume (cm^3) was measured by the displacement method every 2 days since Day 1. When the fruit floated on the water, fruits were placed into a container with water to some degree, and manually pressed with a tip to make the fruit surface just below the water surface (Fig. 2A). The weight at that point was measured by an electronic scale and recorded as the volume of the fruit. On the other hand, when the fruit sank into the water, fruits were put into a container filled with water, and the volume of water poured was measured by a measuring cylinder (Fig. 2B). Fruit density (g/cm^3) was calculated by dividing the weight by volume on each measurement day.

Development of fruit models with the 3D reconstruction method

The 3D measurement was carried out every 2 days by Phenotron-MobileScanner (TAIWAN HIPOINT CORP., Kaohsiung, Taiwan), starting on Day 2. Its depth field of view was 65°× 40°, and its resolution was 1,280×720. 'Red Fairy' avocado fruit was horizontally set on a clay-made base at the center of a rotating table, and its shape was captured by the 3D scanner while rotated 360°, producing a total of 277 models (Fig. 3). Then, the unnecessary point clouds from the base and table were removed with MeshLab ver. 2021.05. In order to calculate the volume of developed fruit models with Python ver. 3.8, ball-pivoting function and Poisson reconstruction function in the Python Open3D

doi:10.6342/NTU202302656

library ver. 0.17.0 were utilized. Ball-pivoting algorithm, a computational geometry algorithm, was applied to the developed model to reduce the surface noise caused by the 3D scanner (Bernardini et al., 1999). Besides, since the lower half and most upper part of the model was missing due to the self-occlusion and unsuitable capturing angles (Fig. 4A), the Poisson reconstruction method was utilized to fit a watertight surface from the original point clouds (Fig. 4B) (Kazhdan et al., 2006; Kazhdan and Hoppe, 2013).

Parameters measured after fruit reached ripening

Fruit DM content (%) was measured in 'Choquette' and 'Hass' after the fruit became ripe, following the previously described method by Melado-Herreros et al. (2021). About 10 g of sliced fruit mesocarp was obtained by a peeler to widely include the mesocarp from near the seed to just below the outer skin. They were placed on a plate and dried at 80 ° C for 8-9 hours in an oven. Once weighed, it was heat-dried for another 2 hours and weighed again. When those weights did not change largely, the secondly measured weight was recorded. When it changed largely, this process was repeated until it was confirmed that the weights did not change. DM content was calculated by the following formula and the average of three replicates per sample was obtained;

$$\%DM = \frac{dried\ flesh\ weight\ (g)}{original\ moist\ flesh\ weight\ (g)}$$

Seed-related characteristics were also evaluated. After removing the seed from the flesh, seed weight was measured by an electronic scale, and its volume was measured by the displacement method. The volume of the seed cavity of the fruit was measured manually by filling it with water, and the weight of water poured into the cavity was recorded as the cavity volume. Seed space volume was defined by subtracting seed volume from seed cavity volume (Fig. 5).

doi:10.6342/NTU202302656

Statistical analysis

Statistical analyses were performed using R version 4.1.2 (R core team 2021). Distribution normality was checked by the Shapiro test and a non-parametric test was done if the p-value was less than 0.05. Regarding the parametric comparisons, Student t-test was done to compare 2 groups and Tukey-Kramer's multiple comparison tests were done for multiple comparisons. On the other hand, Wilcoxon's rank sum test and Steel-Dwass multiple comparison tests (Monte Carlo method) was performed for comparing 2 groups and more than 2 groups non-parametrically, respectively. Principal component analysis (PCA) was also performed on R. Each measured parameter was taken as a variable, and their values were standardized so that the variance became 1.

doi:10.6342/NTU202302656

Results and Discussions

Determination of the definition of ripening

The firmness change in 'Red Fairy' batch 1 is shown in Fig. 6. Firmness continued to drop gradually from the beginning until day 5, where the firmness range among fruit reached the maximum, and drastic change was observed from day 5 to 7, further followed by a slight decline. This trend was consistent with the previous report (Arzate-Vázquez et al., 2011).

There are numerous methods to measure firmness, and definitions of 'ready-to-eat' or 'ripe' depends on the machines or settings used in the experiments. Besides, in avocados, some measured firmness with unpeeled fruit, but others did only for flesh after peeling (Hershkivitz et al., 2009; Kokawa et al., 2020), possibly resulting in different values for the same fruit. Although one of the most often utilized equipment is a penetrometer (Tinyane et al., 2018; Fuentealba et al., 2017), this is destructive in many cases (Hershkivitz et al., 2009), so it may not be suitable for the successive firmness evaluations on the same fruit (Uarrota and Pedreschi, 2022). Besides, hand-squeezing evaluation is also often used (Burdon et al., 2015), yet it was not used in this study because it could not assure objectivity. For those reasons, as far as the author searched, no papers were found in which researchers defined ripeness based on firmness measurement on unpeeled avocado fruits with a texture analyzer, as performed in this study.

Thus, the definition of ripening here was newly set by the author with the turning points from a drastic decrease to a slight decrease in firmness. It was obvious that after the firmness reached below approximately 10 N, its change became small (Fig. 6). Therefore, in this research, the fruit was regarded as ripe when its firmness got below 10 N and proceeded to other measurements, including DM measurement and seed characteristics evaluation.

doi:10.6342/NTU202302656

Ripening traits of each sample batch of three tested avocado cultivars

Table 2 shows a summary of avocado fruit ripening. Average days to ripen were significantly varied even within any cultivars. Especially, its variance was quite huge in 'Hass', ranging from 5.00 days to 14.6 days, which were the shortest and longest average ripening period in this experiment, respectively. Whole fruit density also could be significantly varied within the same cultivars, except in 'Red Fairy'. In addition, whole fruit density at arrival or first measurement and at ripening were significantly high in 'Hass', reaching almost 1.00, but no significant difference was observed between the other 2 cultivars. Comparing at arrival and at ripening, generally, density increased at different degrees, which implied the general trend of increasing density during ripening. DM content was significantly high in 'Hass', originating from the different races with the 'Choquette' of Guatemalan × West Indian, and 'Hass' of Guatemalan × Mexican (Chang et al., 2003).

Besides, the numbers of fruits for each ripening duration are listed in Table 3. The range of ripening duration was smallest in 'Choquette', from 5 to 11 days, but it was broader in 'Red Fairy' from 5 to 15 days and in 'Hass' from 5 days to 19 days.

Changes in measured parameters during ripening

The weight change trend is shown by Fig. 7. Fruits were categorized into groups based on the ripening duration as shown in Table 3, and the changes were represented as the mean weight values with standard errors. In 'Choquette', weight changes were not smooth between Day 1 to Day 3, because some fruits lack measurements on Day 1 due to a shipping issue. Instead, their measurements were included in the data since Day 3, affecting the mean weight values in some categories. Except that, on the whole, weight decreased gradually as the ripening process continued. Weight loss is mainly caused by

doi:10.6342/NTU202302656

respiration and evaporation through micro-cracks, lenticels, and tissue permeation. During respiration, organic compounds are broken down and converted into carbon dioxide, which can go out of the fruit tissues as gas (Lufu et al., 2020).

The volume changes were shown in Fig. 8. Volume measurement on Day 1 failed in ‘Red Fairy’ batch 1 due to technical issues, further failing to calculate density. Therefore, the transitions from Day 1 to Day 3 seemed unstable, which was the same in ‘Choquette’, as described above. The trend looked similar to the weight change, continuing to decrease with ripening days. However, it could be characterized by the relatively sharp decrease in 2 or 4 days before reaching the ripening (Fig. 8). Volume decrease could be driven by the internal air loss and turgor pressure decline. Internal air could be abundant among cells and around the seed, especially in avocado fruit. Turgor pressure decrease is related to water loss from the flesh cells that would be driven by evaporation (Lufu et al., 2020).

The fruit peel color was turned from green to red and black in ‘Red Fairy’ and ‘Hass’, respectively (Fig. 9). However, its color stayed green at ripening in ‘Choquette’, corresponding to the previous report (Arancibia-Guerra et al., 2022; Wu et al., 2023). Changes in color parameters in ‘Red Fairy’, ‘Choquette’, and ‘Hass’, including L*, a*, b*, C*, and h, were represented in Fig. 10, 11, and 12, respectively. On the whole, rapid changes were observed at the latter stages of ripening. Besides, the changes in those color parameters in ‘Choquette’ was relatively slight with the smaller ranges. L*, b*, and C* values decreased in ‘Red Fairy’ and ‘Hass’, but increased in ‘Choquette’ as ripening days passed. This indicated the loss of lightness, yellowness, and chroma in the former 2 cultivars and the opposite trend in ‘Choquette’. a* values also showed the opposite trends among cultivars, indicating the color change from green to red in ‘Red Fairy’ and ‘Hass’,

doi:10.6342/NTU202302656

and the slight loss of redness in ‘Choquette’. h values decreased in ‘Red Fairy’ and ‘Choquette’, but increased in ‘Hass’.

Chronological changes in firmness are represented in Fig. 13. Firmness decreased towards the end of ripening with rapid color change mainly from 2-4 days before ripening, the same as volume and color change.

Fig. 14 shows the chronological changes in density. Matching the results in Table 2, fruit density increased during ripening in all cultivars, characterized by a relatively slight change at the beginning and greater increase at the latter stages. Since weight showed more constant and gradual decrease than volume (Fig. 7 and 8), density increase was thought to be driven mainly by a faster decrease in volume. Although the obvious increasing trend of the whole fruits was observed, the changing trends were different among fruits (Fig. 15). In ‘Red Fairy’, the color of the heatmap changed from light orange to dark orange, which meant that it tended to increase toward ripening. The same trend was observed in ‘Hass’ batch 5 and 6, reaching a maximum density at ripening. However, batch 4 exhibited fluctuating density change. Similarly, in ‘Choquette’, although batch 4 showed a general tendency of density increase toward ripening, batch 3 did not show any certain patterns of change. Those results implied that density dynamics could vary among batches or fruits even within the same cultivar. This may influence the density-ripening relationship in individual fruits.

Results of principal component analysis showing factors that contributed to the ripening

PCA was performed to clarify which factors measured were strongly related to ripening, taking weight, volume, color values of L*, a*, b*, C* and h, firmness, and density from the first measurement and the measurement at ripening as variables. Fig. 16 shows strength of relevance of each parameter to ripening. Basically, in all cultivars, the

doi:10.6342/NTU202302656

changes caused by ripening was mainly represented by PC1 which explained more than 50% of the whole variance, and PC1 increased as ripening proceeded.

In ‘Red Fairy’, firmness was negatively associated with PC1, approximately 180 degrees opposite to a* (Fig. 16A). The other color values, L*, b*, and C* were placed near firmness, negatively related to PC1. On the other hand, h, weight, volume and density were negatively related to PC2, thought to represent the diversity among fruits. Since firmness could be considered to be mostly related to eating quality among those variables, a* value, which was negatively, but most strongly related to firmness and represented the peel color change from green to red, was chosen as the representative color indicator during ripening in ‘Red Fairy’.

Firmness and color indicators were also well related to PC1 in ‘Choquette’ as well (Fig. 16B). Firmness was in the negative direction of PC1, but the placement of color indicators was different from that of ‘Red Fairy’. L*, b* and C* were positioned as a cluster in the positive direction, but a* and h were negative. Weight and volume were positively related to PC2, representing the diversity among fruits. Although density was mainly related to PC2 in a negative direction, but also slightly positively related to PC1. b*, C*, and h were considered to be negatively or positively related to firmness as color indicators, but since the differences between groups of different ripening duration were most clearly shown by b* and C* (Fig. 11), and they showed a very similar trend, b* value was chosen as the representative indicator.

In ‘Hass’, firmness was placed in the negative direction of PC1 along with L*, b*, and C*, while a* and h were placed in the positive direction (Fig. 16C). Although weight, volume and density were basically related to PC2, weight and volume were also negatively related to PC1, and density was positively related to it. As for the color indicator, a* was selected as a representative because it was arrayed almost opposite side

doi:10.6342/NTU202302656

to firmness and it represented well the change in peel color from green to purple or black.

In terms of density, it was orthogonal to firmness in most cases, and seemed to represent diversity among fruits rather than the changes during ripening.

Relationships between density and firmness or color

In order to see if the ripening could be predictable by density, firstly, the relationships between density and firmness or color were investigated. Since fruits from 'Hass' batch 5 presented significantly faster ripening patterns (Table 2) and quite a wide range of densities among fruits (Fig. 17), the fruits from 'Hass' batch 5 were excluded in the sections below. Besides, a fruit from 'Hass' batch 4 was also excluded because its density was too small and regarded as an outlier. Density and firmness, and density and color values from all measurements did not show any correlations (Fig. 18). This was possibly because the range of density difference among fruits was greater than the range of density change during ripening. The average density ranges among fruits at the same time points were 0.120, 0.0640, and 0.0531 in 'Red Fairy', 'Choquette', and 'Hass', respectively. On the other hand, its ranges during ripening were 0.0650, 0.0107, and 0.0318, respectively.

Therefore, it was investigated if the fruit classification based on whole fruit density at the very beginning of storage resulted in sorting fast- and slow-ripening fruit. Fruits were classified into 3 groups, low-density group (LD), medium-density group (MD), and high-density group (HD) based on the result of the first density measurement, so that the number among those groups were almost equal (Table 4). Since density measurement on Day 1 failed in 'Red Fairy' batch 1, fruit density on Day 3 was used. In addition, although there was no density data for the 'Choquette' fruits of batch 3 from Taichung on Day 1, density data on Day 1 from fruits except them was used for the

doi:10.6342/NTU202302656

classification since their number was not so big. Significant differences in density were observed among those 3 groups in every cultivar (Fig. 19). When the fastest fruit reached ripening, differences in firmness or color value among those 3 groups were investigated. In 'Red Fairy' and 'Hass', the HD group had significantly high firmness and low a* value, indicating slower ripening than the lower density group (Fig. 20A and C). On the other hand, in 'Choquette', the HD group had significantly low firmness and a high b* value, indicating fast ripening (Fig. 20B). As the highly matured fruit could be presumed to accumulate much more oil content (Lee et al., 1983), density was considered to be low in those fruits at or just after the harvest (Fig. 1). Considering that most research has shown that the ripening speed becomes faster with the harvest date (Blakey et al., 2009; Burdon et al., 2015), the trend observed in 'Red Fairy' and 'Hass', in which fruit with higher density showed a faster-ripening pattern, was reasonable. Interestingly, however, the opposite trend was found in 'Choquette'. Although the trend varied among cultivars, it succeeded in roughly classifying slow- or fast-ripening fruit based on whole fruit density just after the harvest.

Predictions of ripening parameters based on whole fruit density calculated by the displacement method

Since the approximate trend between density and ripening speed was found, it was explored if the ripening parameters could be predicted precisely from density or not. To confirm this, Spearman's rank correlation analyses were performed between whole fruit density and firmness from different days of ripening (Table 5, 6 and 7). Significant correlations were observed mainly in the early or mid-ripening period. This would be because the firmness change was quite dramatic in the later ripening stage, making the relationship between density and firmness unstable. Although the coefficients were

doi:10.6342/NTU202302656

positive in ‘Red Fairy’ and ‘Hass’ (Table 5 and 7), they were negative in ‘Choquette’ (Table 6), matching the results from fruit classification based on density (Fig. 20). The maximum absolute values of the coefficients were relatively high with the highest in ‘Red Fairy’ at 0.786, followed by ‘Choquette’ at -0.667 and ‘Hass’ at 0.617. Similarly, Spearman’s rank correlation analyses were performed between whole fruit density and color value from different days of ripening (Table 8, 9 and 10). Compared with the correlations between firmness and whole fruit density, significant correlations were observed in fewer cells. Although quite high correlation coefficients were observed in ‘Hass’ at the latter stages, it would be due to the small number of avocado fruits left on Day 17 (n = 6) (Table 10). Besides, correlations observed at the latter stages of ‘Hass’ were positive, as opposed to the negative correlations mostly observed in ‘Hass’. Except for those quite high coefficients, the coefficient with the maximum absolute value was -0.715 in ‘Red Fairy’ (Table 8), 0.439 in ‘Choquette’ (Table 9), and -0.514 in ‘Hass’ (Table 10). Since they were not as high as the ones observed in the correlation to firmness, it was suggested that firmness could be more tightly related to density. Furthermore, the regression models to predict firmness and color from density were established (Table 11 and 12), and the relationships between whole fruit density and firmness where the maximum R-squared was observed (Fig. 21 and 22). However, the maximum R-squared for the firmness prediction was only 0.495 of ‘Red Fairy’ (Table 11) and that for the color prediction was just 0.365 of ‘Red Fairy’ (Table 12). Considering that Hor et al. (2020) succeeded to predict the firmness and color of mango during ripening at the R-squared of 0.65 and 0.83, respectively, those developed regression models may not be feasible for estimating the ripening conditions.

doi:10.6342/NTU202302656

Effect of seed weight and seed space on whole fruit density

The whole fruit density of avocado can be affected by factors other than oil content, such as seed size and density, seed space, or air content in flesh cells (Clark et al., 2007; Self et al.,1994). Fig. 23A and B show the diversity of seed space in 'Red Fairy'. In some fruits, seeds were much smaller than the seed cavity, resulting in big spaces between seed and flesh. However, in others, seeds were tightly adherent to the flesh. Diversity in seed space volume varied among cultivars (Fig. 23C). The ratio of seed space volume to fruit volume was significantly small in 'Hass' compared to the other 2 cultivars. 'Red Fairy' had the widest range of the ratio, ranging from approximately 0 to 0.11. In order to further confirm if the seed size or seed space were independent of fruit size or not, correlation analyses were performed. Seed weight and fruit weight were significantly correlated in 'Choquette' and 'Hass' at coefficients of 0.802 and 0.833, respectively (Fig. 24A). However, no correlation was observed in 'Red Fairy'. On the other hand, seed volume was significantly correlated to fruit volume in all cultivars (Fig. 24B), implying the big diversity of seed density in 'Red Fairy'. As for the seed space, no or quite weak correlations were observed in all cultivars (Fig. 24C). However, due to the quite small ratio of seed space volume to fruit volume in 'Hass' (Fig. 23C), its effect on the whole fruit density in this cultivar was possibly negligible. Furthermore, the ratio of seed weight to fruit weight and that of seed space volume to fruit volume was significantly correlated to the whole density in almost all cultivars, except the latter ratio of 'Hass' (Table 13). Collectively, it has been suggested that diversity in seed weight and seed space volume could affect the whole fruit density.

Therefore, a new density parameter, density subtracting seed size (DS) was established by taking the effect of seed weight and seed volume into consideration. DS on day X (X = 1 to n; n indicates the ripening day) was calculated by the following

doi:10.6342/NTU202302656

formula since seed weight and volume could not be considered to change greatly;

$$DS\ day\ X = \frac{Fruit\ weight\ dayX - seed\ weight\ at\ ripening}{Fruit\ volume\ day\ X - seed\ volume\ at\ ripening}$$

Table 14, 15 and 16 show the result of Spearman's rank correlation analysis between DS and firmness from different days of ripening. Only the relation to firmness was considered because the relationship between density and firmness was better than that to color. Although correlations were still observed in many columns, the maximum absolute values of coefficients in 'Red Fairy' and 'Hass' did not improve compared to the results using the whole fruit density (Table 14 and 16). High correlation coefficients observed in 'Hass' on Day 17 were not considered, because of the small number of fruits left. However, coefficients reached 0.578 on Day 15 with a relatively big sample number of 22, though significant correlations were not observed between whole fruit density and firmness on Day 15. Besides, although the significant correlations observed between DS and firmness on Day 15 and Day 17 were positive, others were negative. The negative relationship indicates that the higher the density, the faster the fruit ripened, which is opposed to the assumed hypothesis in this experiment. However, Fig. 24A and B show that the ratio of seed weight to fruit weight and the ratio of seed volume to fruit volume are somewhat constant among fruits at 'Hass', indicating that seed weight and seed volume are not important factors affecting the whole fruit density diversity in 'Hass'. Therefore, it is possible that the present results of 'Hass' do not need to be taken into account. On the other hand, the maximum absolute value of correlation coefficients increased from -0.667 to -0.694 in 'Choquette', indicating the efficiency of setting a new parameter on this cultivar (Table 15). Compared to the firmness prediction based on whole fruit density, the best R-squared of developed regression models in 'Red Fairy decreased, but it increased in 'Choquette' and 'Hass', reaching 0.449 and 0.420, respectively (Table 17 and Fig. 25). It was, however, still far from practical application.

doi:10.6342/NTU202302656

Another density parameter, density subtracting seed size and space (DC) was also established by further considering the effect of seed space. DC on day X (X = 1 to n; n indicates the ripening day) was calculated by the following formula;

$$DC\ day\ X = \frac{Fruit\ weight\ dayX - seed\ weight\ at\ ripening}{Fruit\ volume\ day\ X - seed\ volume\ at\ ripening - seed\ space\ volume\ at\ ripening}$$

This formula assumes that the seed space does not change a lot in the ripening period, but this may not be true and the seed space volume could decrease during ripening, since the fruit volume has been shown to decrease (Fig. 8). To precisely evaluate the effect of space volume on fruit density, chronological measurement may be required. Table 18, 19 and 20 show the correlation analyses between DC and firmness from different days of ripening. Correlations were found in fewer relations. The absolute values were smaller than those observed in relation to the whole fruit density and firmness with maximums of 0.518 in 'Red Fairy' (Table 18), -0.613 in 'Choquette' (Table 19), and -0.489 in 'Hass' (Table 20). Although the seed space volume and its diversity among fruit apparently affected whole fruit density, taking them into consideration did not improve their relationship.

Potential factors weakening relationships between density and ripening

Relationships among maturity, ripening, and density revealed in this study are summarized in Fig. 26. Although it failed to develop feasible regression models to estimate precise ripening statuses, fruits were classified into faster- or slower-ripening groups based on the fruit density just after the harvest or before ripening. While whole fruit density showed a general increasing trend with smaller ranges than density diversity among fruits, density changes in individual fruits were diverse among fruits. Besides, even though 2 density parameters, DS and DC were considered to reflect the flesh density

doi:10.6342/NTU202302656

better than whole fruit density, their relations to ripening were almost equivalent to whole fruit density or much weaker in most cases. Therefore, it was implied that flesh density and ripening were not correlated very much. This could be due to the lack of a strong correlation between oil content and flesh density, so the correlation between %DM and DC at ripening was investigated in 'Choquette' and 'Hass'. However, no or quite weak significant correlations were observed (Fig. 27). Clark et al. (2007) attributed the gap between %DM and flesh density to the diversity in internal airspace and the composition of oil lipids in the flesh, which can be supported by the observations by Self et al. (1994). They demonstrated that the density and air content of avocado flesh was highly correlated with $r = 0.954$ in their regression.

Besides, Hofman et al. (2000) reported that the increase in fruit DM during maturity was slight in late-harvested 'Hass' and highlighted that the relationship between DM and maturity was much more obvious during the early harvesting period. In this research, fruits from 3 cultivars were considered late-harvested. Therefore, it is possible that fruit maturity was not mirrored in %DM, thus weakening the correlation between density and ripening.

Comparison of relations of whole fruit density and firmness during ripening with respect to firmness

Conventionally, firmness has been one of the most often used indicators for ripening prediction. People often held or squeezed the avocado fruit by hand and determined ripening stages or predicted how many days required for full-ripeness (Gamble et al., 2010). Therefore, two types of relationships, whole fruit density and firmness, to firmness during ripening were compared.

Table 21, 22 and 23 show the correlations between firmness and firmness from

doi:10.6342/NTU202302656

different days of ripening in ‘Red Fairy’, ‘Choquette’, and ‘Hass’, respectively. Generally, firmness measured on one day was most correlated with firmness on the next measurement two days later, and decreased with time passed. Since the firmness changes drastically during ripening, the correlation coefficients were thought to reach the highest with the measurement 2 days later perhaps with the smallest changes in firmness, then the correlation was considered to decrease gradually as the change became larger. Besides, correlation coefficients were on the whole higher in ‘Red Fairy’ or ‘Hass’, than in ‘Choquette’, maybe because the ripening proceeded quicker in ‘Choquette’ with the maximum ripening duration of only 11 days (Table 3), making the firmness change more rapid. On the other hand, in ‘Hass’, due to the slower ripening with gentle change in firmness, firmness measured on one day had correlations with firmness measured relatively later.

Comparing the density-firmness relationships with this firmness-firmness relationships, basically the former showed smaller absolute value of correlation coefficients. Besides, density measured on a given day did not necessarily correlate well with firmness on days closer to that day. Although the density-firmness relationships were generally inferior to the firmness-firmness relationships, the absolute values of correlation coefficients were higher in some cases. In ‘Red Fairy’, relations of density Day 1 to firmness on Day 5 and 7 was beyond those of firmness, and in ‘Choquette’, there was significant correlations between density and firmness where the firmness-firmness relationships were not significant. Therefore, basically, relationships of firmness-firmness are superior to those of density-firmness, but the latter may prevail depending on the cultivars and in some cases.

doi:10.6342/NTU202302656

Comparison of volume measurement by the displacement method and the 3D reconstruction method

After the filling by the ball-pivoting method and Poisson reconstruction method, the 3D models developed at the first measurement on 'Red Fairy' batch 1 included an average of 2,072 points per cm^2 of surface area. The 3D reconstruction was tested in 'Red Fairy' if they can replace the conventional displacement method or not. Fig. 28 shows the relationship between volume measured by the displacement method and that by the 3D reconstruction method. They had quite a high R-squared of 0.988, indicating the feasibility of the 3D reconstruction method. The volume measured by the 3D reconstruction method seemed to be bigger than that by the displacement method. This would be attributed to the increased width and length in the former method (Fig. 29). Since the fruit volume gradually decreased during ripening, fruit width and length on day 2 were supposed to slightly decrease compared to those measured on day 1. However, those measured by the 3D reconstruction method were bigger. This indicates that it may be difficult to capture precise fruit shape or volume by this method, but as long as the relationship between actual and predicted volume is constant, it will be able to replace the displacement method in this research.

The relationship between ripening speed and fruit classification based on density measured by the 3D reconstruction method

Fruit classification based on the density measured by the displacement method succeeded in roughly sorting fast- or slow-ripening fruits (Fig. 20). Therefore, it was explored whether the 3D reconstruction method takes it over. Sixty-one 'Red Fairy' fruits were divided into LD (0.797-0.879 g/cm^3, n = 20), MD (0.879-0.904 g/cm^3, n = 21), and HD (0.904-0.958 g/cm^3, n = 20) based on the density evaluated by the 3D reconstruction

doi:10.6342/NTU202302656

method on Day 2. The results were similar to the ones using the displacement method. HD group had significantly higher firmness and lower a* value on Day 7, indicating slower ripening (Fig. 30B and C). Since a significant difference in density was not observed in MD and HD groups (Fig. 30A), the difference in firmness became ambiguous.

Predictions of ripening parameters based on whole fruit density calculated by the 3D reconstruction method

Correlation analyses were performed to see the relationships between firmness or color, and whole fruit density measured by the 3D reconstruction method (Table 24 and 25). Since the weight measurement of fruit from batch 2 failed on Day 8, decreased number of samples affected the correlation analysis, making the relationship of predicted density on day 8 to firmness from other days unanalyzable. The maximum absolute values of coefficients were observed between density on Day 2 and firmness or a* value on Day 5, which was the day where maximum absolute value of coefficients was observed between those parameters and the whole fruit density by the displacement method (Table 5 and 8). Therefore, the similar trend was observed here, too. However, generally correlation coefficients were much smaller compared to the relationships with density by the displacement method. Although the volume measured by two different kinds of methods were quite similar as shown above, subtle differences in volume by these two different methods could affect the correlations, which might be precise and sensitive.

In light of those results, the 3D reconstruction method has the potential to replace the displacement method. As mentioned above, the disadvantages of the displacement method are that it is time-consuming and prone to errors and that fruits need to be wiped out thoroughly afterward in order to remove the moisture on the surface. In this experiment, a single measurement takes less than 30 seconds to create 3D models with

doi:10.6342/NTU202302656

some missing parts, so the time required is small and there is no need for subsequent care. Although the volume itself was larger than the actual value in this filling method (Fig. 29), the ratio of the volume is approximately constant among fruits (R^2 = 0.988, Fig. 28), and it can be used without problems in sorting based on density as in this case.

doi:10.6342/NTU202302656

Conclusions

Avocado fruit is known for its variant and short shelf life. To deal with the postharvest loss of avocados, this study aimed to predict the ripening status non-destructively using density as a parameter. This hypothesis was based on the estimation that highly mature fruit would have lower density and ripe faster since the oil content in avocado was demonstrated to increase with harvest date. In addition, as an effective density measurement method, 3D reconstruction-based volume estimation was proposed.

Density tended to increase in most fruits during ripening, but some showed decreasing trend and others even fluctuated. However, it was not observed that factors such as volume affected those patterns, and what will exactly affect the density dynamics was not identified. Fruit classification based on whole fruit density revealed the differences in ripening speed among different density groups. Although the fruits of 'Red Fairy' and 'Hass' matched the hypothesis that fruit with high density showed slow ripening, those of 'Choquette' displayed the opposite trend. The factor that made 'Choquette' unique should be investigated in the future.

Regression analyses were performed to predict the ripening parameters such as firmness and color based on whole fruit density, but those R-squared were as low as less than 0.5, which was supposed to be far from the practical use. Even though the factors including seed size, volume, and seed space, which were considered to affect the whole fruit density, were excluded, the relationships between density and ripening parameters decreased or slightly increased and did not lead to the dramatic increase in R-squared values. Several possible reasons behind this were stated. Firstly, possibly due to the variance in inner airspace, strong correlations between %DM and density were not observed. Furthermore, it has also been reported that at the later harvesting stage, high maturity did not always accompany the continuous increase in oil content.

doi:10.6342/NTU202302656

Next, two types of volume measurements were compared. The volumes measured by the displacement and 3D reconstruction methods exhibited high similarity, highlighting the high practicability of the 3D reconstruction-based volume measurement. Fruit classifications based on density calculated by the 3D reconstruction method showed a similar trend to the ones by the displacement method, in which the higher density group had a slow ripening tendency. Those results confirmed the feasibility of the 3D reconstruction method in roughly classifying fast-ripening and slow-ripening avocado fruits, although the correlation to firmness or color values were worse than those with the displacement method.

The avocado fruit categorization into LD, MD, and HD based on density could benefit the optimization of the supply chain. If the approximate ripening speeds are similar within a batch, it is possible to supply products that meet the customers' demand, improving the customer experience. This would be effective not only for domestic distribution but also for export. Shipped avocados are placed on the shelf at the retailers' shops with a color chart to let consumers know the best time to eat when they are ready to eat. Our results showed that the avocado fruits may be roughly classified into different ripening speeds by fruit density. They could be packed according to the density at the packinghouses in exporting countries, thus sorting after the simultaneous ripening treatment will be much easier and requires much less labor and time in importing countries. Besides, especially with the case of cultivars other than 'Hass', those gradings could be useful at retailers' shops, helping them prioritizing which fruits to sell first.

doi:10.6342/NTU202302656

References

Ahmed, D.M., A.R. Yousef and H.S.A. Hassan. 2010. Relationship between electrical conductivity, softening and color of Fuerte avocado fruits during ripening. Agriculture and Biology Journal of North America. 1:878-885.

Andaur, J.E., A.R. Guesalaga, E.E. Agosin, M.W. Guarini and P. Irarrázaval. 2004. Magnetic resonance imaging for nondestructive analysis of wine grapes. J. Agric. Food Chem. 52:165–170.

Arancibia-Guerra, C., G. Núñez-Lillo, A. Cáceres-Mella, E. Carrera, C. Meneses, N. Kuhn and R. Pedreschi. 2022. Color desynchronization with softening of 'Hass' avocado: Targeted pigment, hormone and gene expression analysis. Postharvest Biol. Technol. 194:112067.

Arzate-Vázquez, I., J.J. Chanona-Pérez, M.D.J. Perea-Flores, G. Calderón-Domínguez, M.A. Moreno-Armendáriz, H. Calvo, S. Godoy-Calderón, R. Quevedo and G. Gutiérrez-López. 2011. Image processing applied to the classification of avocado variety Hass (*Persea americana* Mill.) during the ripening process. Food Bioprocess Technol. 4:1307-1313.

Aubert, C., G. Chalot, S. Lurol, A. Ronjon and V. Cottet. 2019. Relationship between fruit density and quality parameters, levels of sugars, organic acids, bioactive compounds and volatiles of two nectarine cultivars, at harvest and after ripening. Food Chem. 297:124954.

Awad, T.S., H.A. Moharram, O.E. Shaltout, D.Y.M.M Asker and M.M. Youssef. 2012. Applications of ultrasound in analysis, processing and quality control of food: A review. Food Res. Int. 48:410-427.

Bennett, A.B., G.M. Smith and B.G. Nichols. 1987. Regulation of climacteric respiration in ripening avocado fruit. Plant Physiol. 83:973-976.

doi:10.6342/NTU202302656

Bergh, B. and N. Ellstrand. 1986. Taxonomy of the avocado. California Avocado Society Yearbook, 70: 135-146.

Bernardini, F., J. Mittleman, H. Rushmeier, C. Silva and G. Taubin. 1999. The ball-pivoting algorithm for surface reconstruction. IEEE Trans. Vis. Comput. Graph. 5:349-359.

Blakey, R.J., J.P. Bower and I. Bertling. 2009. Influence of water and ABA supply on the ripening pattern of avocado (*Persea americana* Mill.) fruit and the prediction of water content using Near Infrared Spectroscopy. Postharvest Biol. Technol. 53:72-76.

Bora, P.S., N. Narain, R.V. Rocha and M.Q. Paulo. 2001. Characterization of the oils from the pulp and seeds of avocado (cultivar: Fuerte) fruits. Grasas Aceites. 52:171-174.

Bozokalfa, M.K. and M. Kilic. 2010. Mathematical modeling in the estimation of pepper (*Capsicum annuum* L.) fruit volume. Chil. J. Agric. Res. 70:626-632.

Burdon, J., N. Lallu, G. Haynes, K. Francis, M. Patel, T. Laurie and J. Hardy. 2013. Relationship between dry matter and ripening time in 'hass' avocado. VI International Conference on Managing Quality in Chains 1091:291-296.

Chen, C., Y.P. Chiang and Y. Pomeranz. 1989. Image analysis and characterization of cereal grains with a laser range finder and camera contour extractor. Cereal Chem. 66:466-470.

Cho, B.H., K. Koyama, E. Olivares Díaz and S. Koseki. 2020. Determination of “Hass” avocado ripeness during storage based on smartphone image and machine learning model. Food Bioproc. Tech. 13:1579-1587.

Clark, C.J., A. White, R.B. Jordan and A.B. Woolf. 2007. Challenges associated with segregation of avocados of differing maturity using density sorting at harvest. Postharvest Biol. Technol. 46:119-127.

Clark, C.J., V.A. McGlone, C. Requejo, A. White and A.B. Woolf. 2003. Dry matter

doi:10.6342/NTU202302656

determination in ‘Hass’ avocado by NIR spectroscopy. Postharvest Biol. Technol. 29:301-308.

Cutting, J.G.M., B.N. Wolstenholme and J. Hardy. 1992. Increasing relative maturity alters the base mineral composition and phenolic concentration of avocado fruit. J. Hortic. Sci. 67: 761-768.

Ernst, A.A. 2012. Interaction of storage, ethylene and ethylene inhibitors on post-harvest quality of ‘Maluma’. South African Avocado Growers’ Association Yearbook 35:34-40

Feng, X., A. Apelbaum, E.C. Sisler and R. Goren. 2000. Control of ethylene responses in avocado fruit with 1-methylcyclopropene. Postharvest Biol. Technol. 20:143-150.

Flitsanov, U., A. Mizrach, A. Liberzon, M. Akerman and G. Zauberman. 2000. Measurement of avocado softening at various temperatures using ultrasound. Postharvest Biol. Technol. 20:279–286.

Fuentealba, C., I. Hernández, I., J.A. Olaeta, B. Defilippi, C. Meneses, R. Campos, S. Lurie, S. Carpentier and R. Pedreschi. 2017. New insights into the heterogeneous ripening in Hass avocado via LC–MS/MS proteomics. Postharvest Biol. Technol. 132:51-61.

Funasho Shoji Co., Ltd. n.d. “Facility”. https://www.funasho-s.co.jp/eng/facility.html Referred on 2023.06.13.

Gaete‐Garretón, L., Y. Vargas‐Hernndez, C. León‐Vidal and A. Pettorino‐Besnier. 2005. A novel noninvasive ultrasonic method to assess avocado ripening. J. Food Sci. 70:187-191.

Gall, H. 1997. A ring sensor system using a modified polar coordinate system to describe the shape of irregular objects. Meas. Sci. Technol. 8:1228.

Gamble, J., F.R. Harker, S.R. Jaeger, A. White, C. Bava, M. Beresford, B. Stubbings, M.

doi:10.6342/NTU202302656

Wohlers, P.J. Hofman, R. Marques and A.Woolf. 2010. The impact of dry matter, ripeness and internal defects on consumer perceptions of avocado quality and intentions to purchase. Postharvest Biol. Technol. 57:35-43.

Hernández, I., C. Fuentealba, J.A. Olaeta, S. Lurie, B.G. Defilippi, R. Campos-Vargas and R. Pedreschi. 2016. Factors associated with postharvest ripening heterogeneity of 'Hass' avocados (*Persea americana* Mill). Fruits. 71:259-268.

Hershkovitz, V., H. Friedman, E.E. Goldschmidt and E. Pesis. 2009. The role of the embryo and ethylene in avocado fruit mesocarp discoloration. J. Exp. Bot. 60:791-799.

Hershkovitz, V., S.I. Saguy and E. Pesis. 2005. Postharvest application of 1-MCP to improve the quality of various avocado cultivars. Postharvest Biol. Technol. 37:252-264.

Hofman, P.J., J. Bower and A. Woolf. 2013. Harvesting, packing, postharvest technology, transport and processing. p.489-540. In: Schaffer, B., B.N. Wolstenholme and A.W. Whiley (eds.). The avocado: botany, production and uses. 2nd Edition. CABI International, Wallingford, UK.

Hofman, P.J., M. Jobin-Décor and J. Giles. 2000. Percentage of dry matter and oil content are not reliable indicators of fruit maturity or quality in late-harvested 'Hass' avocado. HortScience. 35:694-695.

Hor, S., M. Léchaudel, H. Mith and C. Bugaud. 2020. Fruit density: A reliable indicator of sensory quality for mango. Sci. Hortic. 272:109548.

Jaramillo-Acevedo, C.A., W.E. Choque-Valderrama, G.E. Guerrero-Álvarez and C. A. Meneses-Escobar. 2020. Hass avocado ripeness classification by mobile devices using digital image processing and ANN methods. Int. J. Food Eng. 16:20190161.

Jarimopas, B., T. Nunak and N. Nunak. 2005. Electronic device for measuring volume of

doi:10.6342/NTU202302656

selected fruit and vegetables. Postharvest Biol. Technol. 35:25-31.

Jordan, R.B., E.F. Walton, K.U. Klages and R.J. Seelye. 2000. Postharvest fruit density as an indicator of dry matter and ripened soluble solids of kiwifruit. Postharvest Biol. Technol. 20:163-173.

Kazhdan, M. and H. Hoppe. 2013. Screened poisson surface reconstruction. ACM Trans. Graph. 32:1-13.

Kazhdan, M., M. Bolitho and H. Hoppe. 2006. Poisson surface reconstruction. In Proceedings of the fourth Eurographics Symposium on Geometry Processing. 61–70

Khajehdizaj, F.P., A. Taghizadeh and B.B. Nobari. 2014. Effect of feeding microwave irradiated sorghum grain on nutrient utilization, rumen fermentation and serum metabolites in sheep. Livest. Sci. 167: 161-170.

Koc, A.B. 2007. Determination of watermelon volume using ellipsoid approximation and image processing. Postharvest Biol. Technol. 45:366-371.

Kokawa, M., A. Hashimoto, X. Li, M. Tsuta and Y. Kitamura. 2020. Estimation of 'Hass' avocado (*Persea americana* Mill.) ripeness by fluorescence fingerprint measurement. Food Anal. Methods. 13:892-901.

Lee, D.J., R. M. Lane and G. H. Chang. 2001. Three-dimensional reconstruction for high-speed volume measurement. p. 258-267. In: K.G. Harding, J.W.V. Miller and B.G. Batchelor (eds.). Machine vision and three-dimensional imaging systems for inspection and metrology. SPIE, Washington, USA.

Lee, S.K., R.E. Young, P.M. Schiffman and C.W. Coggins. 1983. Maturity studies of avocado fruit based on picking dates and dry weight. J. Am. Soc. Hortic. Sci. 108:390-394.

Lewis, C.E., 1978. The maturity of avocados—a general review. J. Sci. Food Agric. 29:857-866.

doi:10.6342/NTU202302656

Lin, X., H. Zhang, L. Hu, G. Zhao, S. Svanberg and K. Svanberg. 2020. Ripening of avocado fruits studied by spectroscopic techniques. J. Biophotonics. 13:202000076.

Liu, F.W. 1976. Banana response to low concentrations of ethylene. J. Am. Soc. Hortic. Sci. 101:222-224.

Liu, X., J. Sievert, M.L. Arpaia and M.A. Madore. 2002. Postulated physiological roles of the seven-carbon sugars, mannoheptulose, and perseitol in avocado. J. Am. Soc. Hortic. Sci. 127:108-114.

Lorente, D., N. Aleixos, J.U.A.N. Gómez-Sanchis, S. Cubero, O.L. García-Navarrete and J. Blasco. 2012. Recent advances and applications of hyperspectral imaging for fruit and vegetable quality assessment. Food Bioprocess Tech. 5:1121-1142.

Lufu, R., A. Ambaw and U.L. Opara. 2020. Water loss of fresh fruit: Influencing pre-harvest, harvest, and postharvest factors. Sci. Hortic. 272:109519.

Maftoonazad, N., Y. Karimi, H.S. Ramaswamy and S. O. Prasher. 2011. Artificial neural network modeling of hyperspectral radiometric data for quality changes associated with avocados during storage. J Food Process. Preserv. 35:432-446.

Magwaza, L.S. and S.Z. Tesfay. 2015. A review of destructive and non-destructive methods for determining avocado fruit maturity. Food Bioproc. Tech. 8:1995-2011.

Maisl, M., S. Kasperl, S. Oeckl and A. Wolff. 2006. Process monitoring using three dimensional computed tomography and automatic image processing. In Proceedings of the 9th European Conference on Non-Destructive Testing. 1-6.

Mardigan, L., A. Kwiatkowski, J. Castro and E. Clemente. 2014. Application of biofilms on fruits of avocado (*Persea Americana* Miller) in Postharvest. Int. J. Sci. 3:35-45.

McGlone, V.A., R.B. Jordan, R. Seelye and P.J. Martinsen. 2002. Comparing density and NIR methods for measurement of kiwifruit dry matter and soluble solids content. Postharvest Biol. Technol. 26:191-198.

doi:10.6342/NTU202302656

Melado-Herreros, A., S. Nieto-Ortega, I. Olabarrieta, M. Gutiérrez, A. Villar, J. Zufía, N. Gorretta and J.M. Roger. 2021. Postharvest ripeness assessment of 'Hass' avocado based on development of a new ripening index and Vis-NIR spectroscopy. Postharvest Biol. Technol. 181:111683.

Miraei Ashtiani, S.H., A. Salarikia, M.R. Golzarian and B. Emadi. 2016. Non-destructive estimation of mechanical and chemical properties of persimmons by ultrasonic spectroscopy. Int. J. Food Prop. 19:1522-1534.

Mishra, P., M. Paillart, L. Meesters, E. Woltering, A. Chauhan and G. Polder. 2021. Assessing avocado firmness at different dehydration levels in a multi-sensor framework. Infrared Phys. Technol. 118:103901.

Mizrach, A. and U. Flitsanov. 1999. Nondestructive ultrasonic determination of avocado softening process. J. Food Eng. 40:139-144.

Mizrach, A., N. Galili, S. Gan-Mor, U. Flitsanov and I. Prigozin. 1996. Models of ultrasonic parameters to assess avocado properties and shelf life. J. Agric. Eng. Res. 65:261-267.

Mohsenin, N.N. 1970. Physical properties of plant and animal materials. Gordon and Breach Science Publishers, New York, USA.

Moreda, G.P., J. Ortiz-Cañavate, F.J. García-Ramos and M. Ruiz-Altisent. 2009. Non-destructive technologies for fruit and vegetable size determination–a review. J. Food Eng. 92:119-136.

Ncama, K., L.S. Magwaza, C.A. Poblete-Echeverria, H.H. Nieuwoudt, S.Z. Tesfay and A. Mditshwa. 2018. On-tree indexing of 'Hass' avocado fruit by non-destructive assessment of pulp dry matter and oil content. Biosyst. Eng. 174:41-49.

Osondu, H.A.A., S.A. Akinola, T. Shoko, S.K. Pillai and D. Sivakumar. 2022. Coating properties, resistance response, molecular mechanisms and anthracnose decay

doi:10.6342/NTU202302656

reduction in green skin avocado fruit (‘Fuerte’) coated with chitosan hydrochloride loaded with functional compounds. Postharvest Biol. Technol. 186:111812.

Ozdemir, F. and A. Topuz. 2004. Changes in dry matter, oil content and fatty acids composition of avocado during harvesting time and post-harvesting ripening period. Food Chem. 86:79–83.

Pedreschi, R., P. Muñoz, P. Robledo, C. Becerra, B.G. Defilippi, H. van Eekelen, R. Mumm, E. Westra and R.C. De Vos. 2014. Metabolomics analysis of postharvest ripening heterogeneity of ‘Hass’ avocadoes. Postharvest Biol. Technol. 92:172-179.

Pedreschi, R., V. Uarrota, C. Fuentealba, J.E. Alvaro, P. Olmedo, B.G. Defilippi, C. Meneses and R. Campos-Vargas. 2019. Primary metabolism in avocado fruit. Front. Plant Sci. 10:795.

Pesis, E., Y. Fuchs and G. Zauberman. 1978. Cellulase activity and fruit softening in avocado. Plant Physiol. 61:416-419.

Ranney, C. 1991. Relationship between physiological maturity and percent dry matter of avocados. California Avocado Soc. Yrbk. 75:71–85.

Rowell, A.W.G. 1988. Cold storage capacity of avocados from different geographic regions. South African Avocado Growers’ Assn. Yrbk. 11:41-47.

Sacher, J.A. 1962. Relations between changes in membrane permeability and the climacteric in banana and avocado. Nature. 195:577-578.

Schmilovitch, Z., A. Hoffman, H. Egozi, R. El-Batzri and C. Degani. 1997. Determination of avocado maturity by near-infrared spectrometry. In III International Symposium on Sensors in Horticulture 562:175-179.

Self, G.K., E. Ordozgoiti, M.J.W. Povey and H. Wainwright. 1994. Ultrasonic evaluation of ripening avocado flesh. Postharvest Biol. Technol. 4:111-116.

Shezi, S., L.S. Magwaza, S.Z. Tesfay and A. Mditshwa. 2020. Biochemical changes in

doi:10.6342/NTU202302656

response to canopy position of avocado fruit (cv.‘Carmen’and ‘Hass’) during growth and development and relationship with maturity. Sci. Hortic. 265:109227.

Sowmya, V., K.P. Soman and M. Hassaballah. 2019. Hyperspectral image: Fundamentals and advances. p.401-424. In: M. Hassaballah and K.M. Hosny (eds.). Recent Advances in Computer Vision: Theories and Applications. Springer Cham, Cham, Switzerland.

Storey, W.B., B. Bergh and G.A. Zentmyer. 1986. The origin, indigenous range, and dissemination of the avocado. California Avocado Soc. Yrbk. 70:127-133.

Tan, C.X. 2019. Virgin avocado oil: An emerging source of functional fruit oil. J. Funct. Foods. 54:381-392.

Teng, S.W., H. Tung-Chuan, J.J. Shyr and A. Wakana. 2016. Lipid content and fatty acid composition in Taiwan avocados (*Persea americana* Mill). J. Fac. Agr., Kyushu Univ., 61: 65–70.

Tinyane, P.P., P. Soundy and D. Sivakumar. 2018. Growing ‘Hass’ avocado fruit under different coloured shade netting improves the marketable yield and affects fruit ripening. Sci. Hortic. 230:43-49.

Uarrota, V.G. and R. Pedreschi. 2022. Mathematical modelling of Hass avocado firmness by using destructive and non-destructive devices at different maturity stages and under two storage conditions. Folia Hortic. 34:139-150.

Wang, M., Y. Xu, Y. Yang, B. Mo, M.A. Nikitina and X. Xiao. 2022. Vis/NIR optical biosensors applications for fruit monitoring. Biosens. Bioelectron. X:100197.

Wang, W. and C. Li. 2014. Size estimation of sweet onions using consumer-grade RGB-depth sensor. J. Food Eng. 142:153-162.

Wang, W., T.R. Bostic and L. Gu. 2010. Antioxidant capacities, procyanidins and pigments in avocados of different strains and cultivars. Food Chem. 122:1193-1198.

doi:10.6342/NTU202302656

Wedding, B.B., C. Wright, S. Grauf and R.D. White. 2012. The application of near infrared spectroscopy for the assessment of avocado quality attributes. p.211-230. In: T. Theophanides (ed.). Infrared Spectroscopy - Life and Biomedical Sciences. InTechOpen, London, UK.

Woolf, A., C. Clark, E. Terander, V. Phetsomphou, R. Hofshi, M.L. Arpaia, D. Boreham, M. Wong and A. White. 2003. Measuring avocado maturity; ongoing developments. The Orchidardist. 40-45.

Woolf, A.B., I.B. Ferguson, L.C. Requejo-Tapia, L. Boyd, W.A. Laing and A. White. 1999. Impact of sun exposure on harvest quality of 'Hass' avocado fruit. Rev. Chapingo Ser. Hortic. 5:353-358.

Wu, C.J., M.C. Lin and H.F. Ni. 2023. *Colletotrichum* species causing anthracnose disease on avocado fruit in Taiwan. Eur. J. Plant Pathol. 165: 629-647.

Wu, H., C. Chou, T.L. Chang and I.Z. Chen. 2007. Genetic relationship estimation of Taiwan avocado cultivars by volatile constituents of leaves. In Proceedings VI World Avocado Congress, Viña del Mar, Chile:12-16.

Xi, W., Y. Liu, W. Zhao, R. Hu and X. Luo. 2021. Colored radiative cooling: How to balance color display and radiative cooling performance. Int. J. Therm. Sci. 170: 107172.

Yokohama Customs. 2021. "Avocado-no-yunyu". https://www.customs.go.jp/yokohama/toukei/topics/data/2109avocado.pdf. Referred on 2023. 06. 13. In Japanese.

Zhang, J., X. Wang, J. Xia, S. Xing and X. Zhang. 2022. Flexible sensing enabled intelligent manipulator system (FSIMS) for avocados (*Persea Americana* Mill) ripeness grading. J. Clean. Prod. 132599.

doi:10.6342/NTU202302656

Table 1. Summary of avocado samples and storage conditions in the present study

Cultivar	Red Fairy		Choquette				Hass		
Batch	1	2	3	3	3	4	4	5	6
Harvest date	Nov. 22, 2022	Dec. 5, 2022	Dec. 27, 2022	Dec. 27, 2022	Dec. 27, 2022	Feb. 8, 2023	Feb. 8, 2023	Feb. 14, 2023	Feb. 22, 2023
Origin	Chiayi	Taichung	Yunlin	Chiayi	Taichung	Chiayi	Chiayi	Taichung	Taichung
Number of fruits	31	30	16	16	17	15	20	20	27
Average storage temperature (°C)	23.0	21.1	22.9	22.9	22.9	22.9	22.8	23.0	22.7
Average storage relative humidity (%)	88.0	87.1	83.0	83.0	83.0	85.6	82.6	81.2	80.3

doi:10.6342/NTU202302656

Table 2. Ripening traits of each sample batch of three tested avocado cultivars

Cultivar	Red Fairy		Choquette				Hass		
Batch	1	2	3	3	3	4	4	5	6
Days to ripen (days)	7.52 b*	9.27 a	8.25 ab	6.50 c	7.59 bc	9.00 a	12.3 b	5.00 c	14.6 a
Density at arrival or first measurement (g/cm^3)	0.945 a	0.943 a	0.950 ab	0.952 ab	0.960 a	0.937 b	0.985 b	0.989 ab	1.00 a
	0.944 b		0.950 b				0.993 a		
Density at ripening (g/cm^3)	0.965 a	0.950 a	0.947 b	0.961 a	0.965 a	0.946 b	0.990 b	1.01 ab	1.02 a
	0.958 b		0.955 b				1.01 a		
Dry matter content (%)	-	-	19.8 a	17.5 b	16.2 b	21.0 a	34.6 b	32.9 b	40.3 a
	-		18.6 b				36.4 a		

* Different letters indicate significant differences at $p < 0.05$ by either the Student t-test, Tukey-Kramer's multiple comparison test, Wilcoxon's rank sum test, or Steel-Dwass multiple comparison test (Monte Carlo method).

doi:10.6342/NTU202302656

Table 3. Time required for ripening and number of fruits in the three cultivars

Required duration	Cultivar		
	Red Fairy	Choquette	Hass
5 days (Rip_dur_05)	1	11	21
7 days (Rip_dur_07)	34	19	2
9 days (Rip_dur_09)	17	31	-
11 days (Rip_dur_11)	3	3	5
13 days (Rip_dur_13)	4	-	17
15 days (Rip_dur_15)	2	-	16
17 days (Rip_dur_17)	-	-	5
19 days (Rip_dur_19)	-	-	1

The abbreviation under days in the cells of required duration is a category that includes all the fruits that reached ripening on that day, and corresponds to the ones that will appear in the figures that follow.

doi:10.6342/NTU202302656

Table 4. Density ranges of low-density, medium-density, and high-density groups

Range of density (g/cm^3)	Cultivar		
	Red fairy	Choquette	Hass
Low-density (LD)	0.872-0.934 (n = 20)	0.917-0.940 (n = 15)	0.984-0.995 (n = 15)
Medium-density (MD)	0.934-0.954 (n = 21)	0.941-0.953 (n = 16)	0.996-1.002 (n = 16)
High-density (HD)	0.957-1.002 (n = 20)	0.954-0.974 (n = 16)	1.002-1.014 (n = 15)

doi:10.6342/NTU202302656

Table 5. Spearman's rank correlation coefficients between density and firmness from different days of ripening in 'Red Fairy'

	Firmness						
Density	Day1	Day3	Day5	Day7	Day9	Day11	Day13
Day1	0.468**	0.681**	0.786**	0.572**	n.s.	n.s.	n.s.
Day3		0.371**	0.470**	0.441**	n.s.	n.s.	n.s.
Day5			0.408**	0.395**	n.s.	n.s.	n.s.
Day7				0.308*	n.s.	n.s.	n.s.
Day9					n.s.	n.s.	n.s.
Day11						n.s.	n.s.
Day13							n.s.

Asterisks indicate the significance at $p < 0.05$ (*) and $p < 0.01$ (**), and n.s. represents that there was no significant correlation. The column highlighted in gray indicates the maximum absolute value of correlation coefficients observed.

doi:10.6342/NTU202302656

Table 6. Spearman's rank correlation coefficients between density and firmness from different days of ripening in ‘Choquette’

	Firmness					
Density	Day1	Day3	Day5	Day7	Day9	Day11
Day1	n.s.	n.s.	-0.440**	-0.563**	-0.438*	n.s.
Day3		n.s.	n.s.	-0.450**	n.s.	n.s.
Day5			-0.363**	-0.472**	n.s.	n.s.
Day7				-0.667**	n.s.	n.s.
Day9					n.s.	n.s.
Day11						n.s.

Asterisks indicate the significance at $p < 0.05$ (*) and $p < 0.01$ (**), and n.s. represents that there was no significant correlation. The column highlighted in gray indicates the maximum absolute value of correlation coefficients observed.

doi:10.6342/NTU202302656

Table 7. Spearman's rank correlation coefficients between density and firmness from different days of ripening in 'Hass'

	Firmness								
Density	Day1	Day3	Day5	Day7	Day9	Day11	Day13	Day15	Day17
Day1	0.577**	0.614**	0.617**	0.406**	0.389**	n.s.	n.s.	n.s.	n.s.
Day3		0.510**	0.498**	0.294*	n.s.	n.s.	n.s.	n.s.	n.s.
Day5			0.603**	0.463**	0.447**	0.351*	n.s.	n.s.	n.s.
Day7				0.394**	0.463**	0.306*	0.346*	n.s.	n.s.
Day9					0.459**	n.s.	n.s.	n.s.	n.s.
Day11						n.s.	0.333*	n.s.	n.s.
Day13							n.s.	n.s.	n.s.
Day15								n.s.	n.s.
Day17									n.s.

Asterisks indicate the significance at $p < 0.05$ (*) and $p < 0.01$ (**), and n.s. represents that there was no significant correlation. The column highlighted in gray indicates the maximum absolute value of correlation coefficients observed.

doi:10.6342/NTU202302656

Table 8. Spearman's rank correlation coefficients between density and a* value of color value from different days of ripening in ‘Red Fairy’

	a* value						
Density	Day1	Day3	Day5	Day7	Day9	Day11	Day13
Day1	-0.591**	-0.666**	-0.715**	-0.562**	n.s.	n.s.	n.s.
Day3		-0.520**	-0.422**	n.s.	n.s.	n.s.	n.s.
Day5			-0.410**	n.s.	n.s.	n.s.	n.s.
Day7				n.s.	n.s.	n.s.	n.s.
Day9					n.s.	n.s.	n.s.
Day11						n.s.	n.s.
Day13							n.s.

Asterisks indicate the significance at $p < 0.05$ (*) and $p < 0.01$ (**), and n.s. represents that there was no significant correlation. The column highlighted in gray indicates the maximum absolute value of correlation coefficients observed.

doi:10.6342/NTU202302656

Table 9. Spearman's rank correlation coefficients between density and b* value of color value from different days of ripening in 'Choquette'

	b* value					
Density	Day1	Day3	Day5	Day7	Day9	Day11
Day1	n.s.	n.s.	0.357*	0.439**	0.405*	n.s.
Day3		n.s.	n.s.	n.s.	n.s.	n.s.
Day5			n.s.	n.s.	n.s.	n.s.
Day7				n.s.	n.s.	n.s.
Day9					n.s.	n.s.
Day11						n.s.

Asterisks indicate the significance at $p < 0.05$ (*) and $p < 0.01$ (**), and n.s. represents that there was no significant correlation. The column highlighted in gray indicates the maximum absolute value of correlation coefficients observed.

doi:10.6342/NTU202302656

Table 10. Spearman's rank correlation coefficients between density and a* value of color value from different days of ripening in ‘Hass’

	a* value								
Density	Day1	Day3	Day5	Day7	Day9	Day11	Day13	Day15	Day17
Day1	n.s.	n.s.	n.s.	-0.494**	-0.385*	n.s.	n.s.	n.s.	n.s.
Day3		n.s.	n.s.	-0.404**	n.s.	n.s.	n.s.	n.s.	n.s.
Day5			n.s.	-0.488**	-0.463**	-0.421**	-0.326*	n.s.	0.943*
Day7				-0.514**	-0.439**	-0.354*	-0.349*	n.s.	n.s.
Day9					-0.438**	-0.352*	n.s.	0.449*	n.s.
Day11						-0.313*	n.s.	n.s.	n.s.
Day13							n.s.	n.s.	n.s.
Day15								n.s.	n.s.
Day17									0.886*

Asterisks indicate the significance at $p < 0.05$ (*) and $p < 0.01$ (**), and n.s. represents that there was no significant correlation. The column highlighted in gray indicates the maximum absolute value of correlation coefficients observed.

doi:10.6342/NTU202302656

Table 11. The best regression models for firmness prediction with the highest R-squared

	Cultivar		
	Red Fairy	Choquette	Hass
Density	Day 1 (D1)	Day7 (D7)	Day 1 (D1)
Firmness	Day 5 (F5)	Day 7 (F7)	Day 5 (F5)
Formula	F-value=27.5**, R^2=0.495, F5 = 167 D1 -127	F-value=34.9**, R^2=0.406, F7 = -224 D7 +226	F-value=20.3**, R^2=0.315, F5 = 488 D1 -452

Asterisks indicate the significance at $p < 0.05$ (*) and $p < 0.01$ (**).

doi:10.6342/NTU202302656

Table 12. The best regression models for color prediction with the highest R-squared

	Cultivar		
	Red Fairy	Choquette	Hass
Density	Day 1 (D1)	Day1 (D1)	Day 1 (D1)
Color	a* Day 3 (a3)	b* Day 9 (b9)	a* Day 7 (a7)
Formula	F-value=16.1**, R^2=0.365, a3 = -47.4 D1 +32.9	F-value=6.44*, R^2=0.205, b9 = 168 D1 -133	F-value=12.9**, R^2=0.227, a7 = 226 D1 -219

Asterisks indicate the significance at $p < 0.05$ (*) and $p < 0.01$ (**).

doi:10.6342/NTU202302656

Table 13. Correlation coefficients between whole fruit density, seed size, and seed space at ripening

	Cultivar		
	Red fairy	Choquette	Hass
Seed weight/ fruit weight	0.624**	0.543**	0.702**
Seed space volume/fruit volume	-0.936**	-0.467**	n.s.

Asterisks indicate significant correlations at $p < 0.01$ (**), and n.s. represents no significant correlation.

doi:10.6342/NTU202302656

Table 14. Spearman's rank correlation coefficients between density subtracting seed size (DS) and firmness from different days of ripening in ‘Red Fairy’

	Firmness						
DS	Day1	Day3	Day5	Day7	Day9	Day11	Day13
Day1	0.461*	0.653**	0.742**	0.487**	n.s.	n.s.	n.s.
Day3		n.s.	n.s.	n.s.	n.s.	n.s.	n.s.
Day5			0.304*	n.s.	n.s.	n.s.	n.s.
Day7				n.s.	n.s.	n.s.	n.s.
Day9					-0.510**	n.s.	n.s.
Day11						n.s.	n.s.
Day13							n.s.

DS on day X was calculated by the formula of (fruit weight on day X – seed weight at ripening) / (fruit volume on day X – seed volume at ripening). Asterisks indicate the significance at $p < 0.05$ (*) and $p < 0.01$ (**), and n.s. represents that there was no significant correlation. The column highlighted in gray indicates the maximum absolute value of correlation coefficients observed.

doi:10.6342/NTU202302656

Table 15. Spearman's rank correlation coefficients between density subtracting seed size (DS) and firmness from different days of ripening in ‘Choquette’

	Firmness					
DS	Day1	Day3	Day5	Day7	Day9	Day11
Day1	n.s.	n.s.	-0.491**	-0.512**	-0.697**	n.s.
Day3		n.s.	n.s.	-0.316**	-0.458**	n.s.
Day5			-0.352**	-0.350*	-0.531**	n.s.
Day7				-0.622**	-0.538**	n.s.
Day9					-0.481**	n.s.
Day11						n.s.

DS on day X was calculated by the formula of (fruit weight on day X – seed weight at ripening) / (fruit volume on day X – seed volume at ripening). Asterisks indicate the significance at $p < 0.05$ (*) and $p < 0.01$ (**), and n.s. represents that there was no significant correlation. The column highlighted in gray indicates the maximum absolute value of correlation coefficients observed.

doi:10.6342/NTU202302656

Table 16. Spearman's rank correlation coefficients between density subtracting seed size (DS) and firmness from different days of ripening in 'Hass'

	Firmness								
DS	Day1	Day3	Day5	Day7	Day9	Day11	Day13	Day15	Day17
Day1	-0.378**	-0.402**	-0.339*	-0.384**	-0.405**	-0.363*	n.s.	n.s.	n.s.
Day3		-0.408**	-0.390**	-0.410**	-0.479**	-0.405**	n.s.	n.s.	n.s.
Day5			n.s.	n.s.	n.s.	n.s.	n.s.	n.s.	n.s.
Day7				n.s.	n.s.	n.s.	n.s.	0.540*	0.943*
Day9					n.s.	n.s.	n.s.	0.578**	n.s.
Day11						n.s.	n.s.	n.s.	n.s.
Day13							n.s.	n.s.	0.943*
Day15								n.s.	0.943*
Day17									n.s.

DS on day X was calculated by the formula of (fruit weight on day X – seed weight at ripening) / (fruit volume on day X – seed volume at ripening). Asterisks indicate the significance at $p < 0.05$ (*) and $p < 0.01$ (**), and n.s. represents that there was no significant correlation. The column highlighted in gray indicates the maximum absolute value of correlation coefficients observed.

doi:10.6342/NTU202302656

Table 17. The best regression models to predict firmness based on density subtracting seed size (DS) for each cultivar

	Cultivar		
	Red Fairy	Choquette	Hass
Density	Day 1 (DS1)	Day 1 (DS1)	Day 9 (DS9)
Firmness	Day 5 (F5)	Day 9 (F9)	Day 15 (F15)
Formula	F-value = 22.7, R^2=0.448**, F5 = 205 DS1 -159	F-value = 20.4, R^2=0.449**, F9 = -114 DS1 +111	F-value =14.5, R^2=0.420**, F15 = 294 D9 -273

DS on day X was calculated by the formula of (fruit weight on day X – seed weight at ripening) / (fruit volume on day X – seed volume at ripening). Asterisks indicate the significance at $p < 0.05$ (*) and $p < 0.01$ (**).

doi:10.6342/NTU202302656

Table 18. Spearman's rank correlation coefficients between density subtracting seed size and space (DC) and firmness from different days of ripening in 'Red Fairy'

	Firmness						
DC	Day1	Day3	Day5	Day7	Day9	Day11	Day13
Day1	0.498**	0.518**	0.385*	0.383*	n.s.	n.s.	n.s.
Day3		0.472*	n.s.	n.s.	n.s.	n.s.	n.s.
Day5			n.s.	n.s.	n.s.	n.s.	n.s.
Day7				n.s.	n.s.	n.s.	n.s.
Day9					n.s.	n.s.	n.s.
Day11						n.s.	n.s.
Day13							n.s.

DC on day X was calculated by the formula of (fruit weight on day X – seed weight at ripening) / (fruit volume on day X – seed volume at ripening – seed space volume at ripening). Asterisks indicate significant correlations at $p < 0.05$ (*), and $p < 0.01$ (**), and n.s. represents that there was no significant correlation. The column highlighted in gray indicates the maximum absolute value of correlation coefficients observed.

doi:10.6342/NTU202302656

Table 19. Spearman's rank correlation coefficients between density subtracting seed size and space (DC) and firmness from different days of ripening in 'Choquette'

	Firmness					
DC	Day1	Day3	Day5	Day7	Day9	Day11
Day1	n.s.	n.s.	-0.370*	-0.345*	-0.492**	n.s.
Day3		n.s.	n.s.	n.s.	n.s.	n.s.
Day5			-0.281*	n.s.	n.s.	n.s.
Day7				-0.613**	-0.379*	n.s.
Day9					-0.444*	n.s.
Day11						n.s.

DC on day X was calculated by the formula of (fruit weight on day X – seed weight at ripening) / (fruit volume on day X – seed volume at ripening – seed space volume at ripening). Asterisks indicate significant correlations at $p < 0.05$ (*), and $p < 0.01$ (**), and n.s. represents that there was no significant correlation. The column highlighted in gray indicates the maximum absolute value of correlation coefficients observed.

doi:10.6342/NTU202302656

Table 20. Spearman's rank correlation coefficients between density subtracting seed size and space (DC) and firmness from different days of ripening in 'Hass'

	Firmness								
DC	Day1	Day3	Day5	Day7	Day9	Day11	Day13	Day15	Day17
Day1	-0.325*	-0.393**	-0.337*	-0.425**	-0.489**	-0.442**	-0.326*	n.s.	n.s.
Day3		-0.393**	-0.351*	-0.403**	-0.467**	-0.360*	n.s.	n.s.	n.s.
Day5			n.s.	n.s.	n.s.	n.s.	n.s.	n.s.	n.s.
Day7				n.s.	n.s.	n.s.	n.s.	0.470*	n.s.
Day9					n.s.	n.s.	n.s.	n.s.	n.s.
Day11						n.s.	n.s.	n.s.	n.s.
Day13							n.s.	n.s.	n.s.
Day15								n.s.	n.s.
Day17									n.s.

DC on day X was calculated by the formula of (fruit weight on day X – seed weight at ripening) / (fruit volume on day X – seed volume at ripening – seed space volume at ripening). Asterisks indicate significant correlations at $p < 0.05$ (*), and $p < 0.01$ (**), and n.s. represents that there was no significant correlation. The column highlighted in gray indicates the maximum absolute value of correlation coefficients observed.

doi:10.6342/NTU202302656

Table 21. Spearman's rank correlation coefficients between firmness and firmness from different days of ripening in 'Red Fairy'

	Firmness						
Firmness	Day1	Day3	Day5	Day7	Day9	Day11	Day13
Day1		0.853**	0.643**	0.550**	n.s.	n.s.	n.s.
Day3			0.711**	0.606*	n.s.	n.s.	0.886*
Day5				0.885**	n.s.	n.s.	n.s.
Day7					0.863**	n.s.	n.s.
Day9						0.867**	n.s.
Day11							0.943*
Day13							

Asterisks indicate significant correlations at $p < 0.05$ (*), and $p < 0.01$ (**), and n.s. represents that there was no significant correlation.

doi:10.6342/NTU202302656

Table 22. Spearman's rank correlation coefficients between firmness and firmness from different days of ripening in 'Choquette'

	Firmness					
Firmness	Day1	Day3	Day5	Day7	Day9	Day11
Day1		0.673**	n.s.	n.s.	-0.647**	n.s.
Day3			0.650**	n.s.	n.s.	n.s.
Day5				0.640**	0.682**	n.s.
Day7					0.799**	n.s.
Day9						n.s.
Day11						

Asterisks indicate significant correlations at $p < 0.05$ (*), and $p < 0.01$ (**), and n.s. represents that there was no significant correlation.

doi:10.6342/NTU202302656

Table 23. Spearman's rank correlation coefficients between firmness and firmness from different days of ripening in 'Hass'

	Firmness								
Firmness	Day1	Day3	Day5	Day7	Day9	Day11	Day13	Day15	Day17
Day1		0.795**	0.708**	0.639**	0.578**	0.417**	n.s.	n.s.	n.s.
Day3			0.900**	0.665**	0.613**	0.469**	0.367*	n.s.	n.s.
Day5				0.741**	0.758**	0.622**	0.523**	n.s.	n.s.
Day7					0.797**	0.701**	0.400*	n.s.	n.s.
Day9						0.806**	0.519**	n.s.	n.s.
Day11							0.771**	n.s.	n.s.
Day13								0.862**	n.s.
Day15									n.s.
Day17									

Asterisks indicate significant correlations at $p < 0.05$ (*), and $p < 0.01$ (**), and n.s. represents that there was no significant correlation.

doi:10.6342/NTU202302656

Table 24. Spearman's rank correlation coefficients between whole fruit density measured by the 3D reconstruction method and firmness from different days of ripening in 'Red Fairy'

	Firmness						
Density	Day1	Day3	Day5	Day7	Day9	Day11	Day13
Day2		n.s.	0.407**	0.343**	n.s.	n.s.	n.s.
Day4			0.330**	n.s.	n.s.	n.s.	n.s.
Day6				0.285**	n.s.	n.s.	n.s.
Day8					n.s.	-	-
Day10						n.s.	n.s.
Day12							n.s.

Asterisks indicate significant correlations at $p < 0.05$ (*), and $p < 0.01$ (**), and n.s. represents that there was no significant correlation. Dashes indicate correlation analysis failed due to the small numbers of data. The column highlighted in gray indicates the maximum absolute value of correlation coefficients observed.

doi:10.6342/NTU202302656

Table 25. Spearman's rank correlation coefficients between whole fruit density measured by the 3D reconstruction method and a* value from different days of ripening in 'Red Fairy'

	a* value						
Density	Day1	Day3	Day5	Day7	Day9	Day11	Day13
Day2		-0.368**	-0.468**	-0.406**	n.s.	n.s.	n.s.
Day4			-0.408**	-0.315*	n.s.	n.s.	n.s.
Day6				-0.310*	n.s.	n.s.	n.s.
Day8					n.s.	-	-
Day10						n.s.	n.s.
Day12							n.s.

Asterisks indicate significant correlations at $p < 0.05$ (*), and $p < 0.01$ (**), and n.s. represents that there was no significant correlation. Dashes indicate correlation analysis failed due to the small numbers of data. The column highlighted in gray indicates the maximum absolute value of correlation coefficients observed.

doi:10.6342/NTU202302656

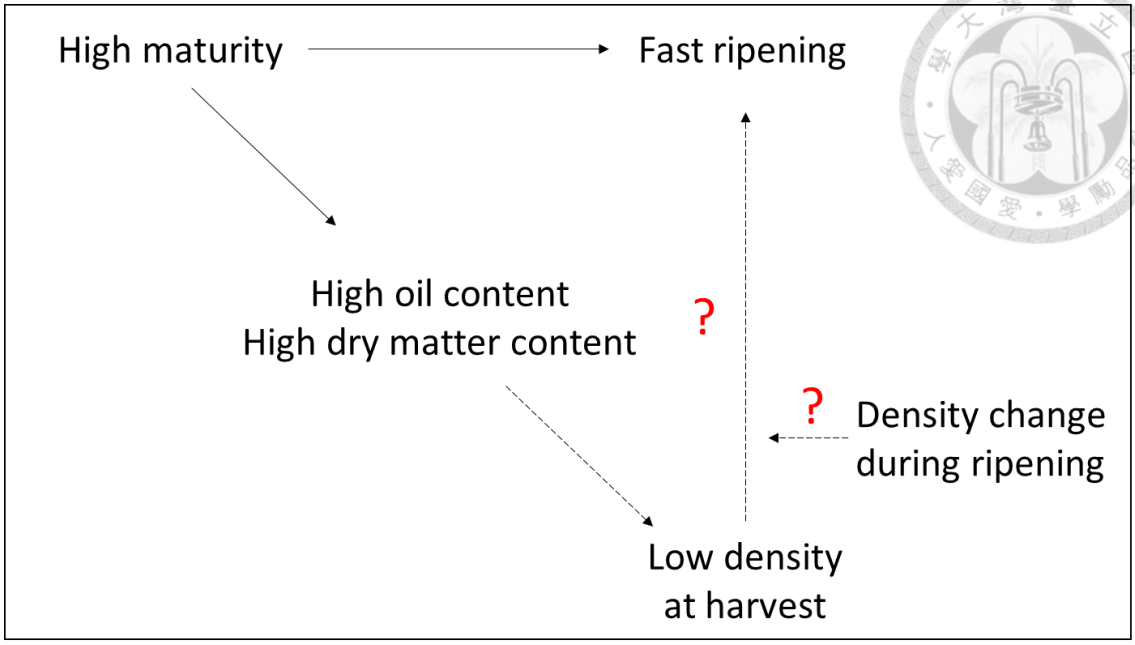

Fig. 1. Hypothesized relationships among maturity, ripening, and density. The intact arrows indicate the relationships reported by previous research. The dotted arrows indicate theoretically possible relationships. In this study, the relationships between ripening and density at harvest, and ripening and density changing during ripening are going to be explored.

doi:10.6342/NTU202302656

A

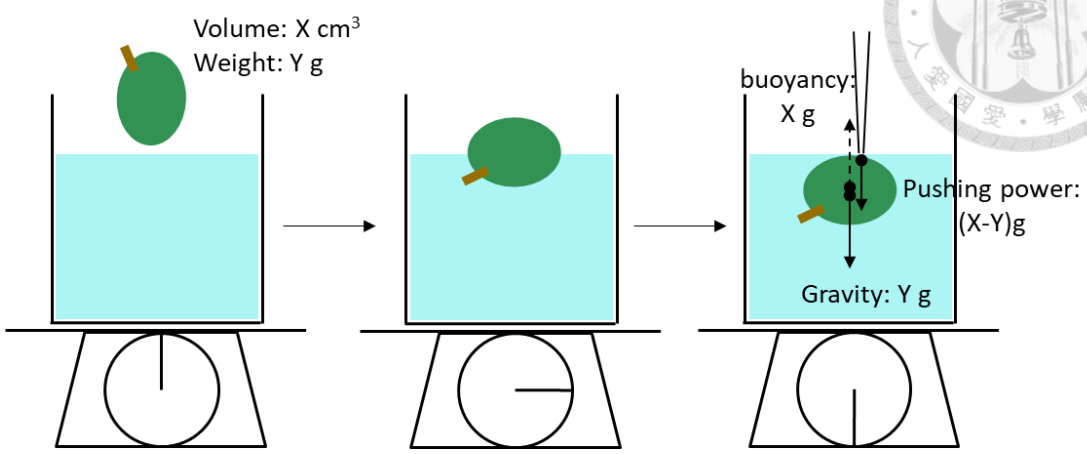

B

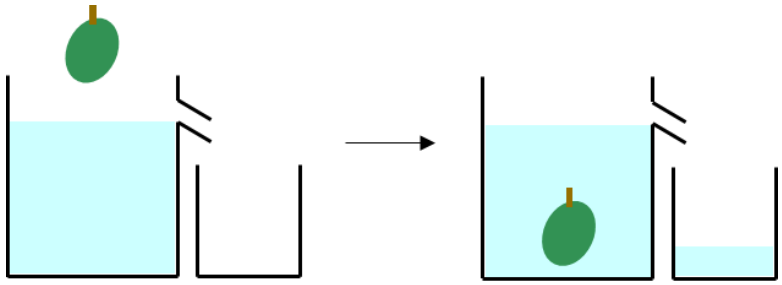

Fig. 2. Two different ways to measure fruit volume. (A) When the fruit floated on the water, the fruit was manually pressed by a tip, and the weight was recorded as the fruit volume at the point when the fruit surface was just below the water's surface. (B) When the fruit sank into the water, the volume of poured water was recorded as the fruit volume.

doi:10.6342/NTU202302656

Fig. 3. Example of the acquisition of a 3D model of an avocado fruit. The fruit was set on the rotating table and its shape was captured by the 3D scanner in the back. A 3D model was reproduced on the computer.

doi:10.6342/NTU202302656

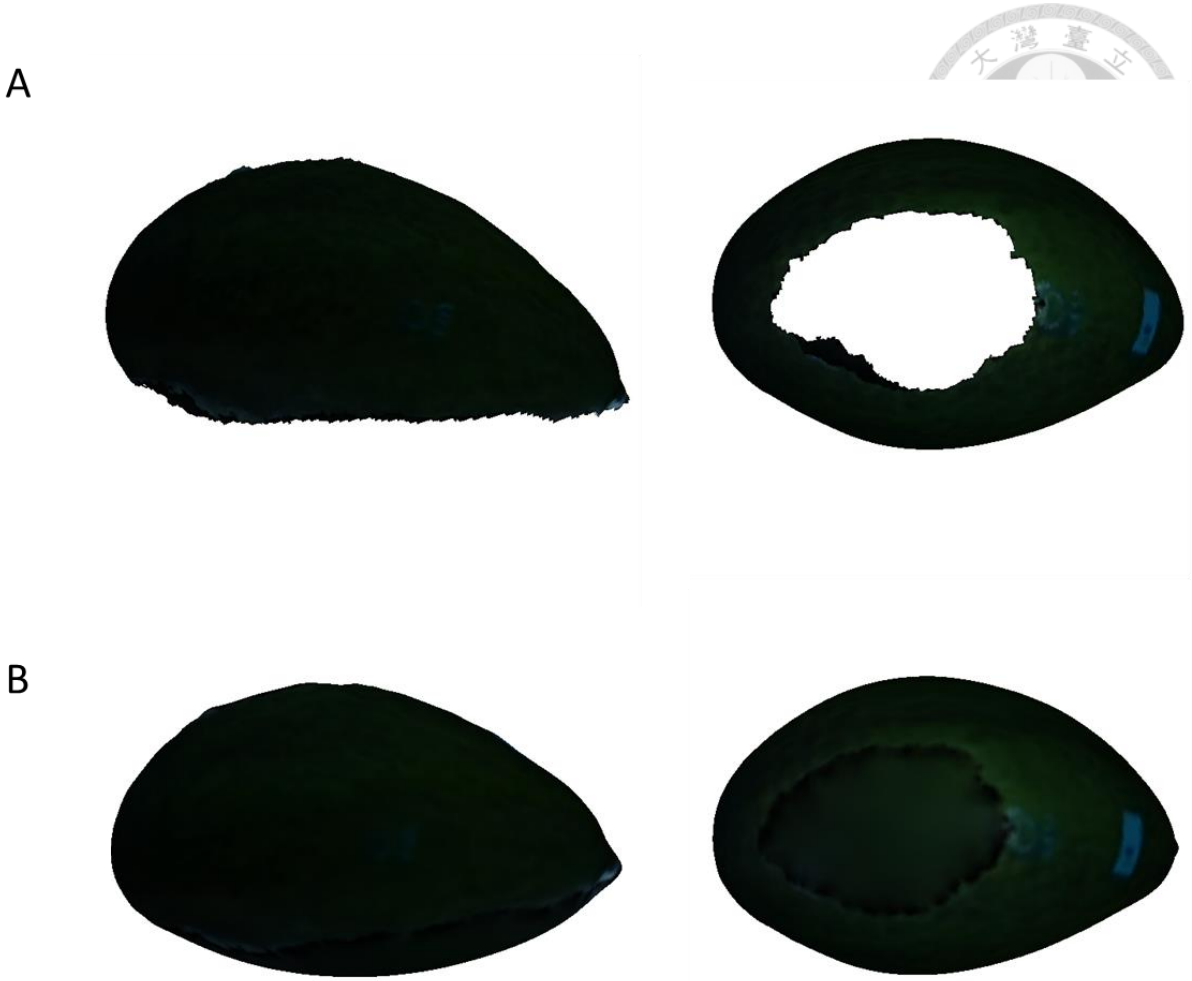

Fig. 4. Examples of developed 3D models. (A) The raw 3D models of laid 'Red Fairy' seen from the side (left) and from above (right). Missing parts can be clearly observed. (B) Filled 3D models after processing by the ball-pivoting method and the Poisson reconstruction method seen from the side (left) and from above (right).

doi:10.6342/NTU202302656

Fig. 5. The definitions of seed cavity and seed space in this study. The seed cavity indicates the hole which appears after the seed is taken out. Seed space indicates the space between the seed cavity and the seed.

doi:10.6342/NTU202302656

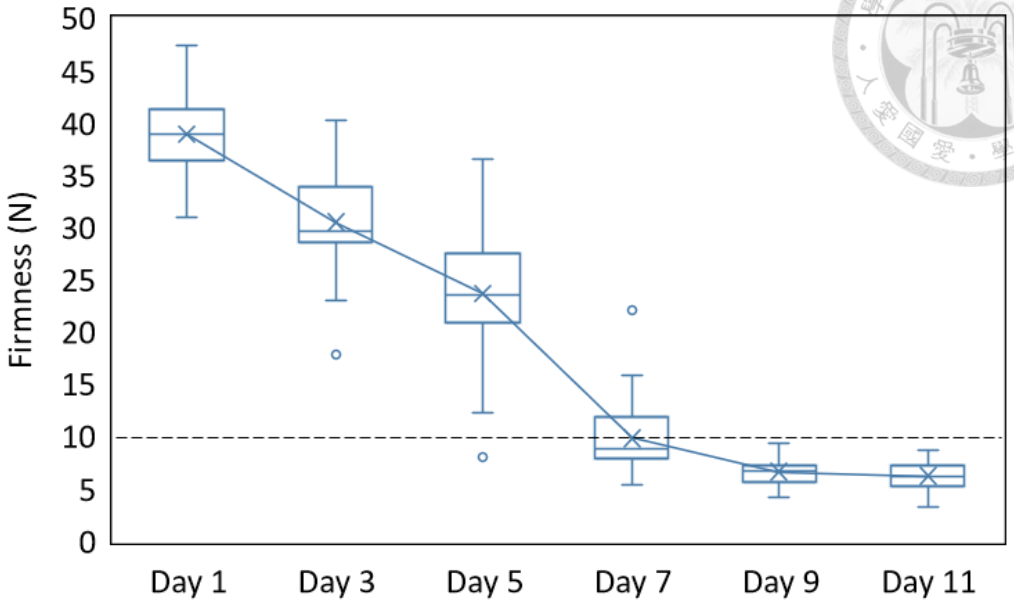

Fig. 6. Firmness changes in ‘Red Fairy’ batch 1 during ripening shown with boxplots (n = 31). The firmness of 10 N is indicated by the dotted line.

doi:10.6342/NTU202302656

A. ‘Red Fairy’

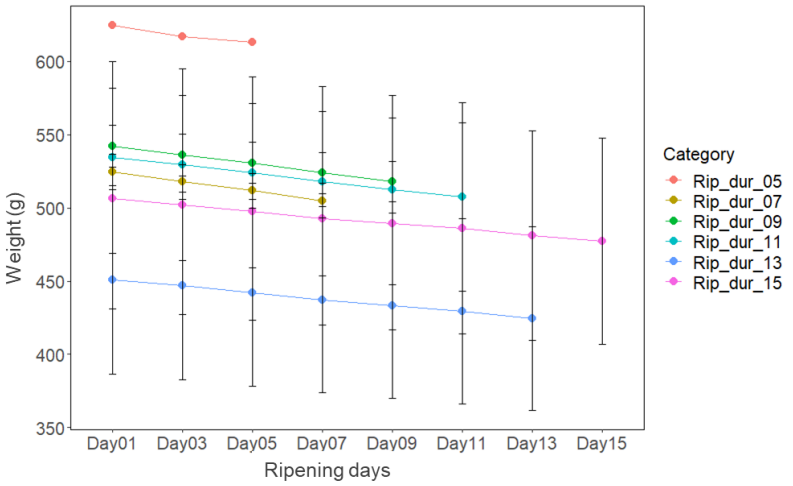

B. ‘Choquette’

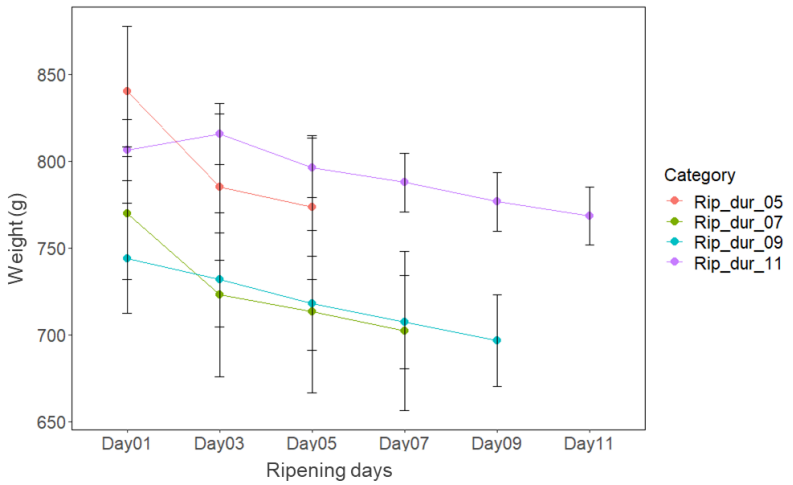

C. ‘Hass’

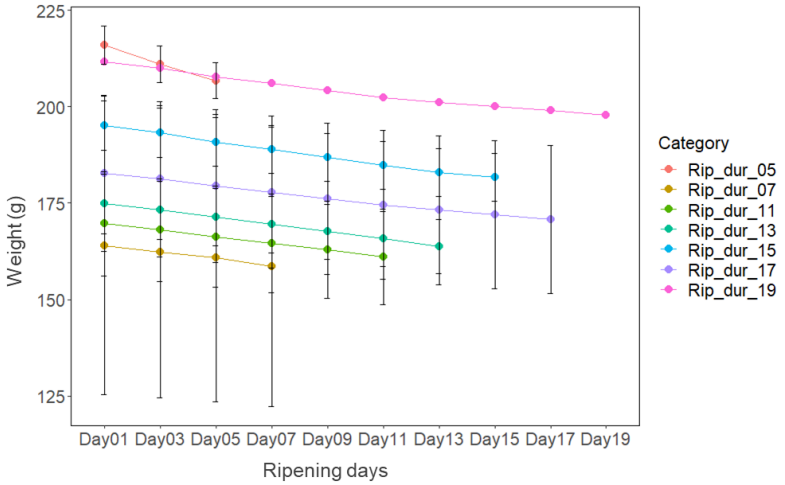

Fig. 7. Weight changes during ripening. Fruits were categorized based on the duration required for ripening. The legends of categories, for example, Rip_dur_05 indicates that the ripening duration was 5 days. Data is represented as the mean values ± S.E.

doi:10.6342/NTU202302656

A. ‘Red Fairy’

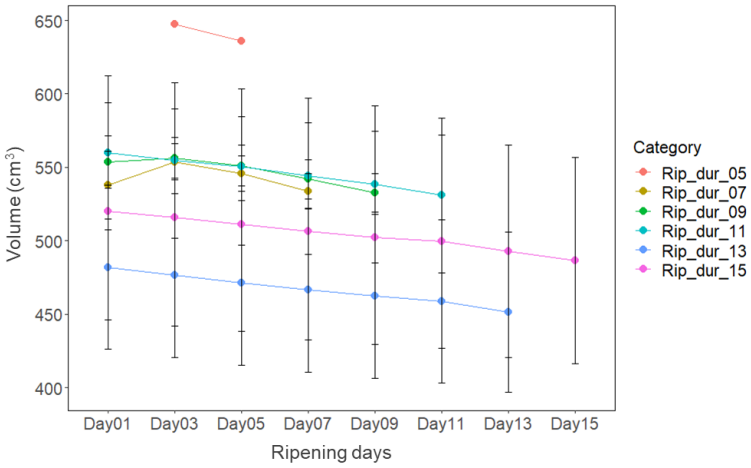

B. ‘Choquette’

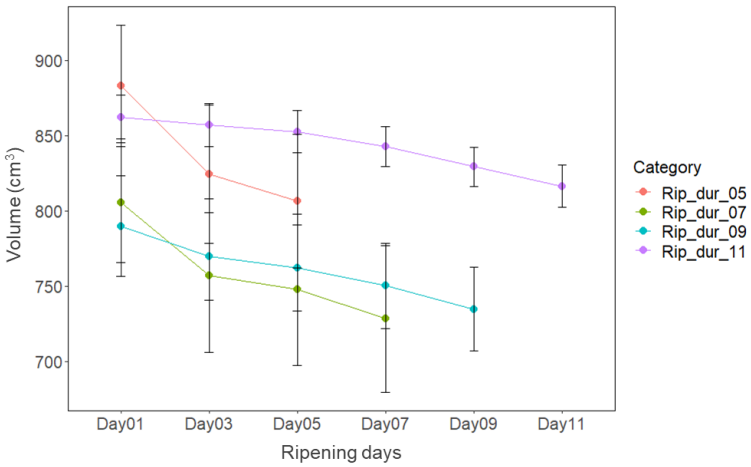

C. ‘Hass’

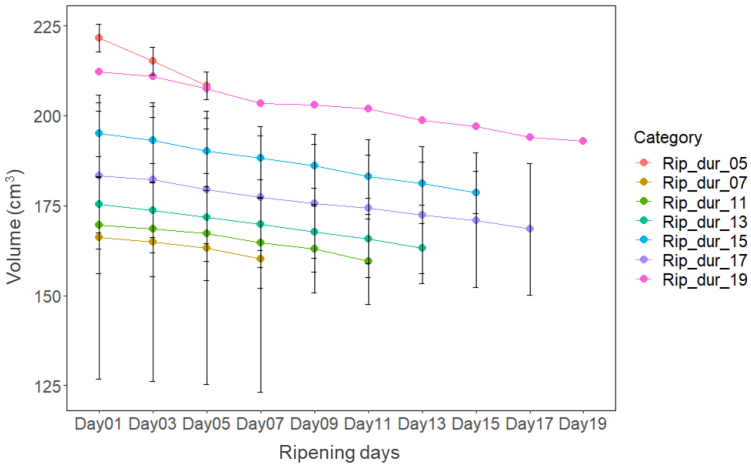

Fig. 8. Volume changes measured by the displacement method during ripening. Fruits were categorized based on the duration required for ripening. The legends of categories, for example, Rip_dur_05 indicates that the ripening duration was 5 days. Data is represented as the mean values ± S.E.

doi:10.6342/NTU202302656

A. ‘Red Fairy’

B. ‘Choquette’

C. ‘Hass’

Day 1 Ripening

Fig. 9. Differences in peel color from Day 1 to ripening in (A) ‘Red Fairy’, (B) ‘Choquette’, and (C) ‘Hass’.

doi:10.6342/NTU202302656

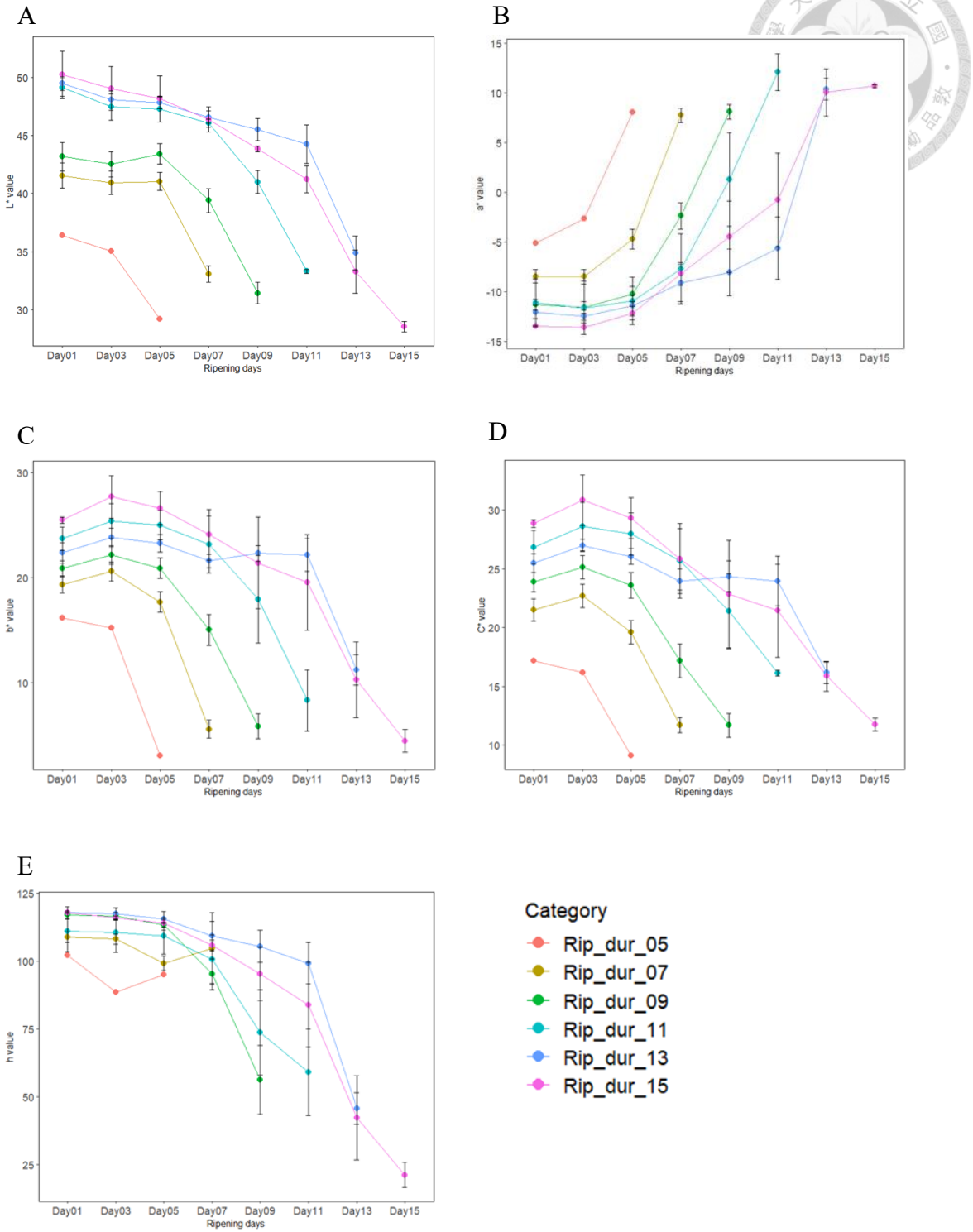

Fig. 10. Changes in color parameters during ripening of 'Red Fairy' fruit. (A) L*, (B) a*, (C) b*, (D) C*, and (E) h value. Fruits were categorized based on the duration required for ripening. The legends of categories, for example, Rip_dur_05 indicates that the ripening duration was 5 days. Data is represented as the mean values ± S.E.

doi:10.6342/NTU202302656

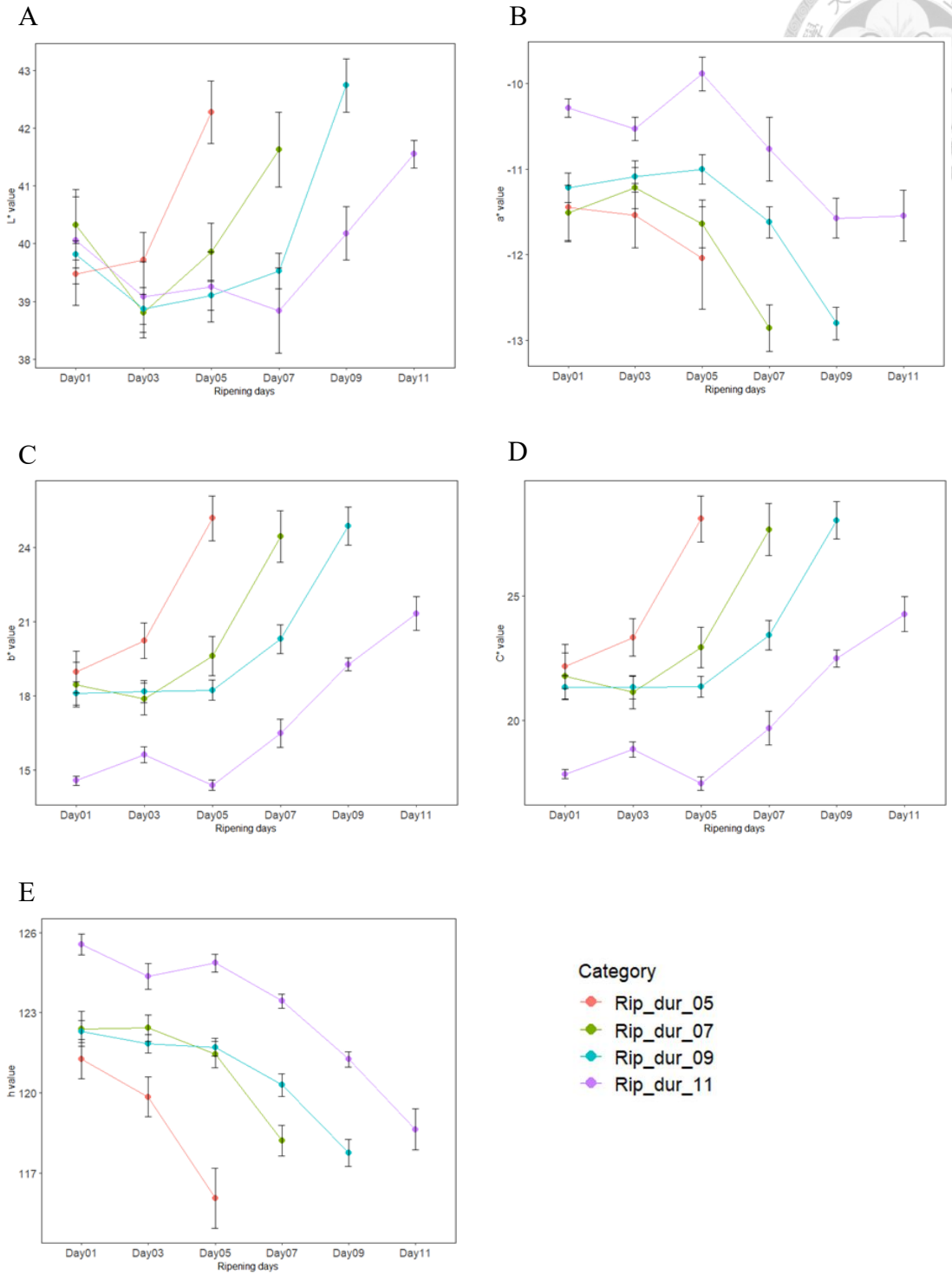

Fig. 11. Changes in color parameters during ripening of 'Choquette' fruit. (A) L*, (B) a*, (C) b*, (D) C*, and (E) h value. Fruits were categorized based on the duration required for ripening. The legends of categories, for example, Rip_dur_05 indicates that the ripening duration was 5 days. Data is represented as the mean values ± S.E.

doi:10.6342/NTU202302656

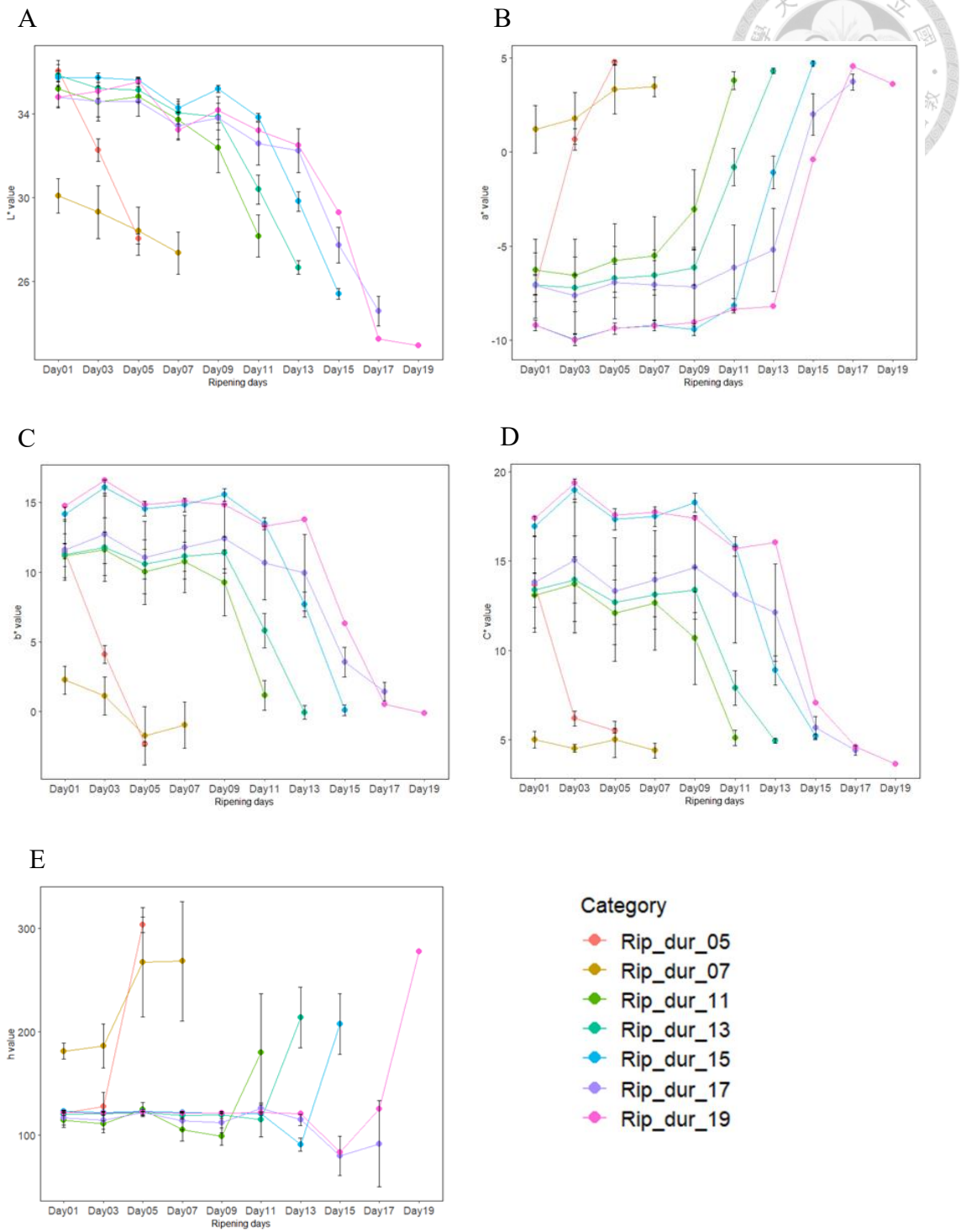

Fig. 12. Changes in color parameters during ripening of 'Hass' fruit. (A) L*, (B) a*, (C) b*, (D) C*, and (E) h value. Fruits were categorized based on the duration required for ripening. The legends of categories, for example, Rip_dur_05 indicates that the ripening duration was 5 days. Data is represented as the mean values ± S.E.

doi:10.6342/NTU202302656

A. ‘Red Fairy’

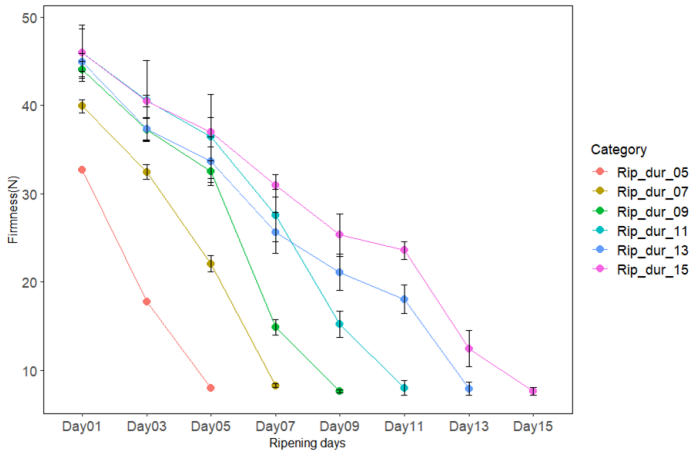

B. ‘Choquette’

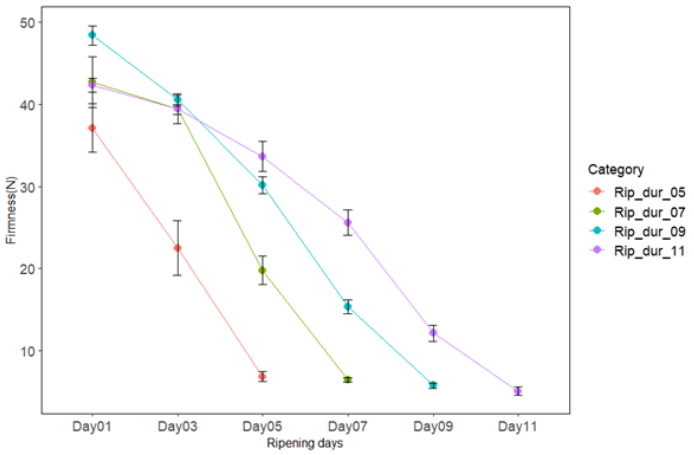

C. ‘Hass’

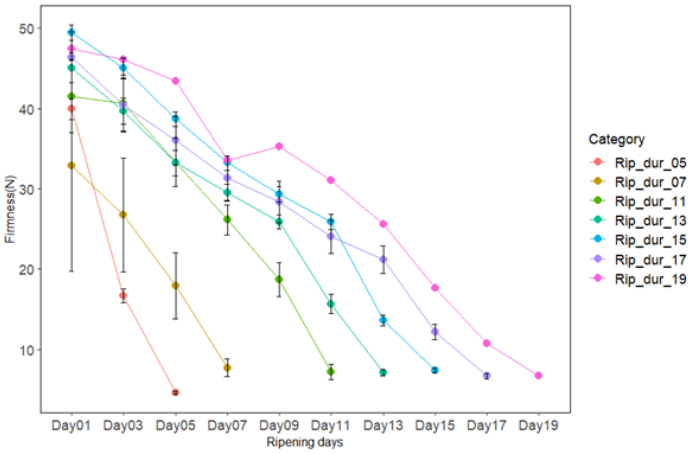

Fig. 13. Firmness changes during ripening. Fruits were categorized based on the duration required for ripening. The legends of categories, for example, Rip_dur_05 indicates that the ripening duration was 5 days. Data is represented as the mean values ± S.E.

doi:10.6342/NTU202302656

A. ‘Red Fairy’

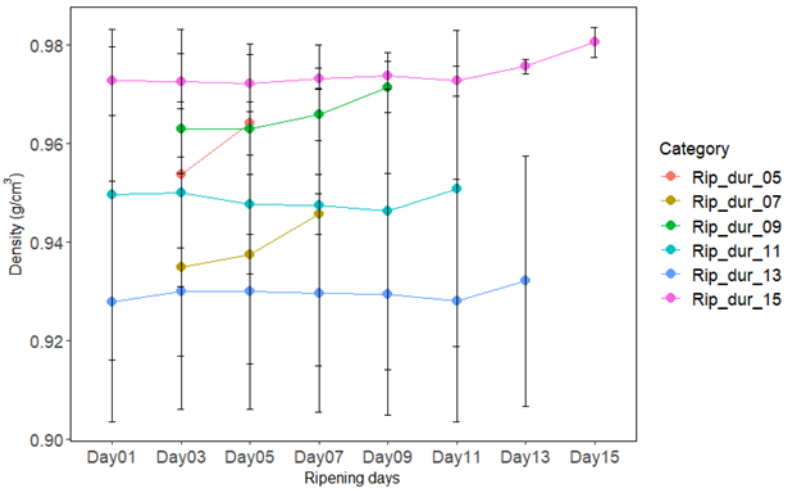

B. ‘Choquette’

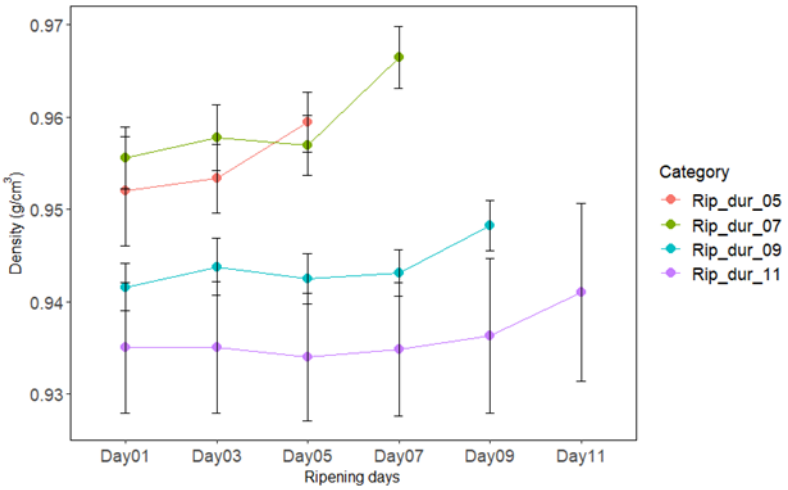

C. ‘Hass’

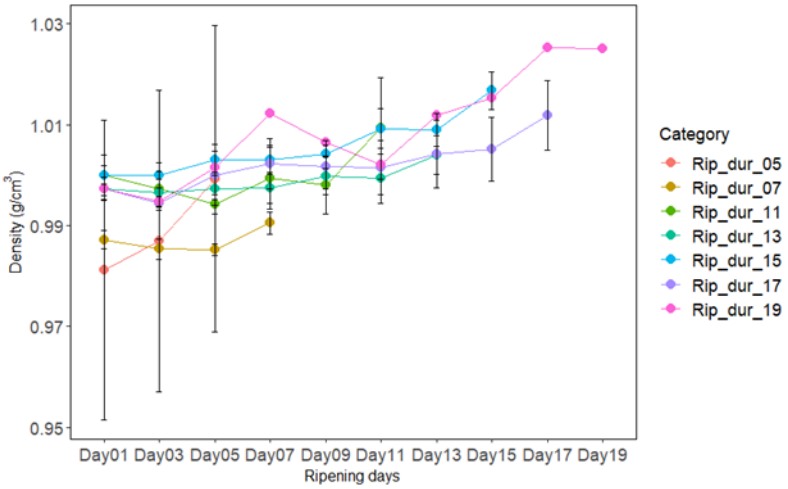

Fig. 14. Density changes during ripening. Fruits were categorized based on the duration required for ripening. The legends of categories, for example, Rip_dur_05 indicates that the ripening duration was 5 days. Data is represented as the mean values ± S.E.

doi:10.6342/NTU202302656

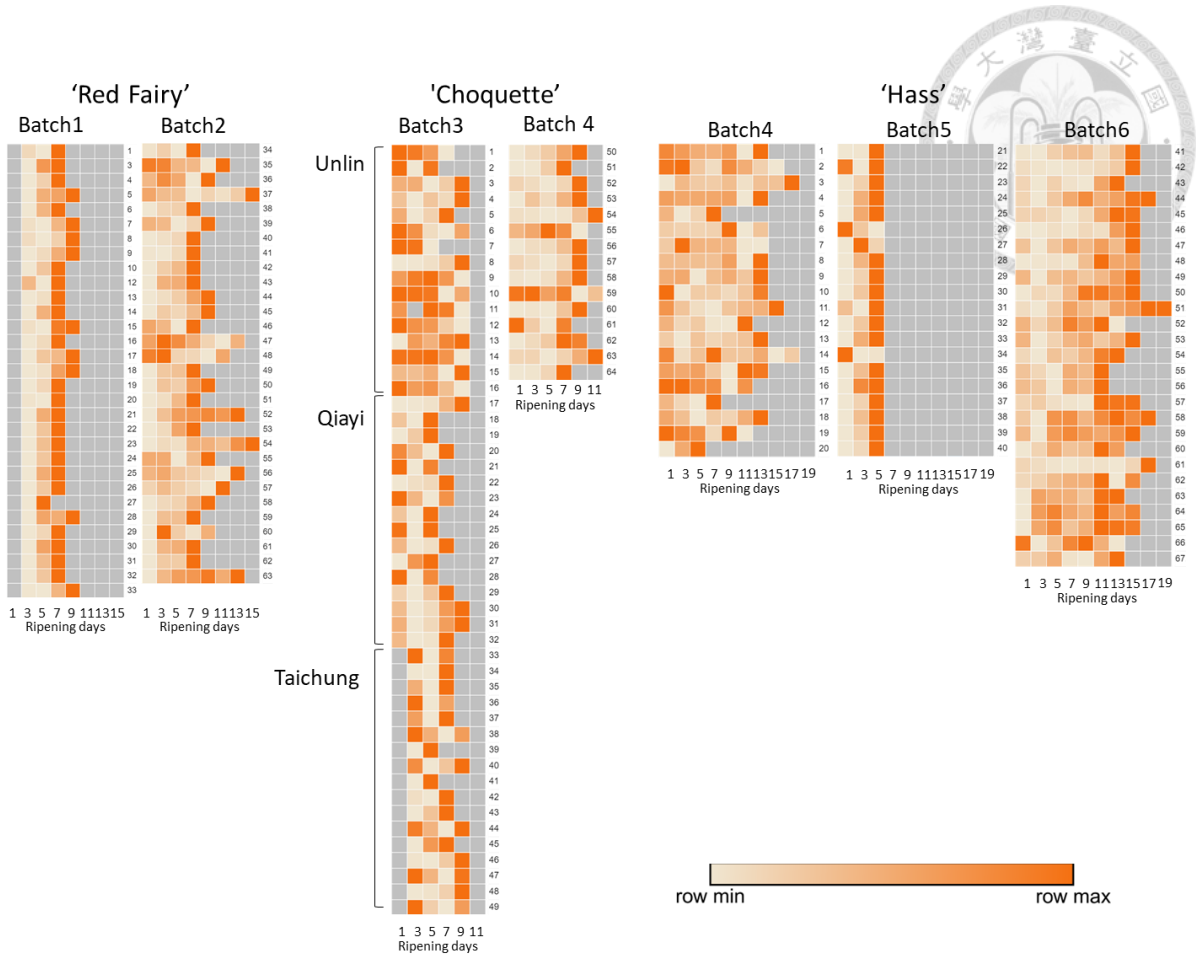

Fig. 15. Heatmap showing density change in the individual fruit during ripening. Dark orange means the maximum density value within a fruit during ripening, and light orange means the minimum density value. Gray cell indicates the absence of data.

doi:10.6342/NTU202302656

A. ‘Red Fairy’

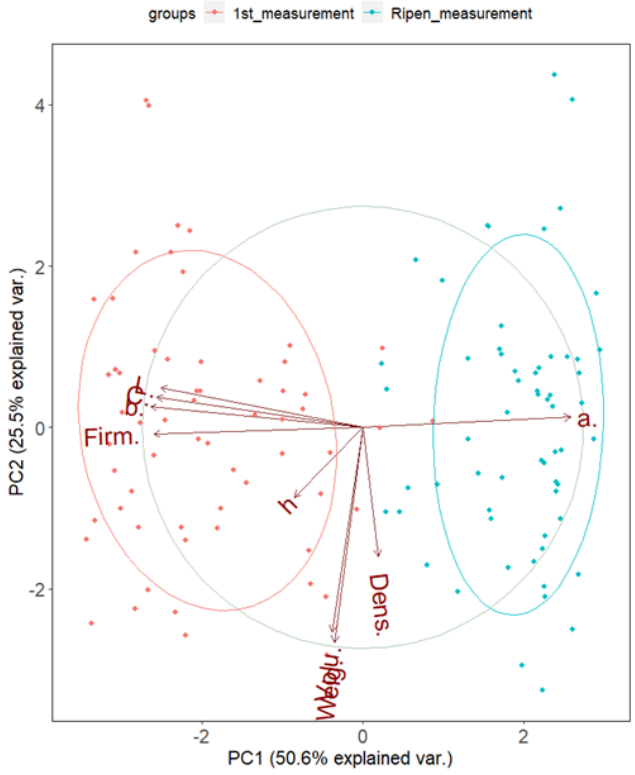

B. ‘Choquette’

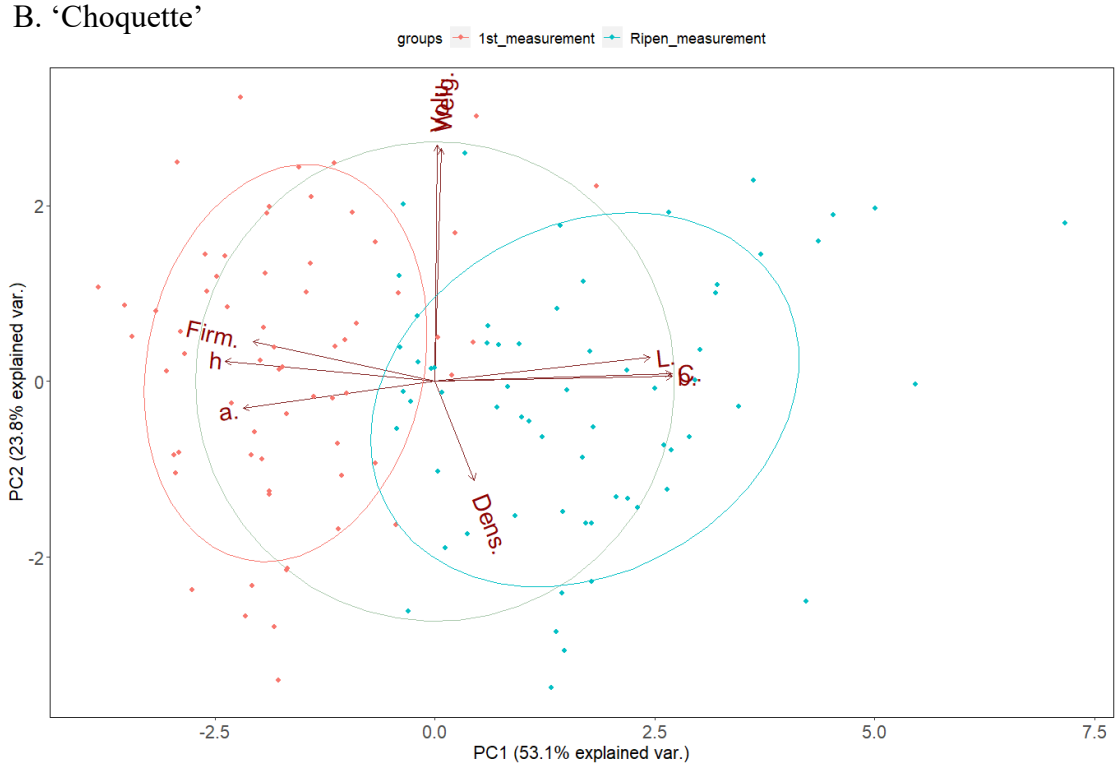

doi:10.6342/NTU202302656

C. ‘Hass’

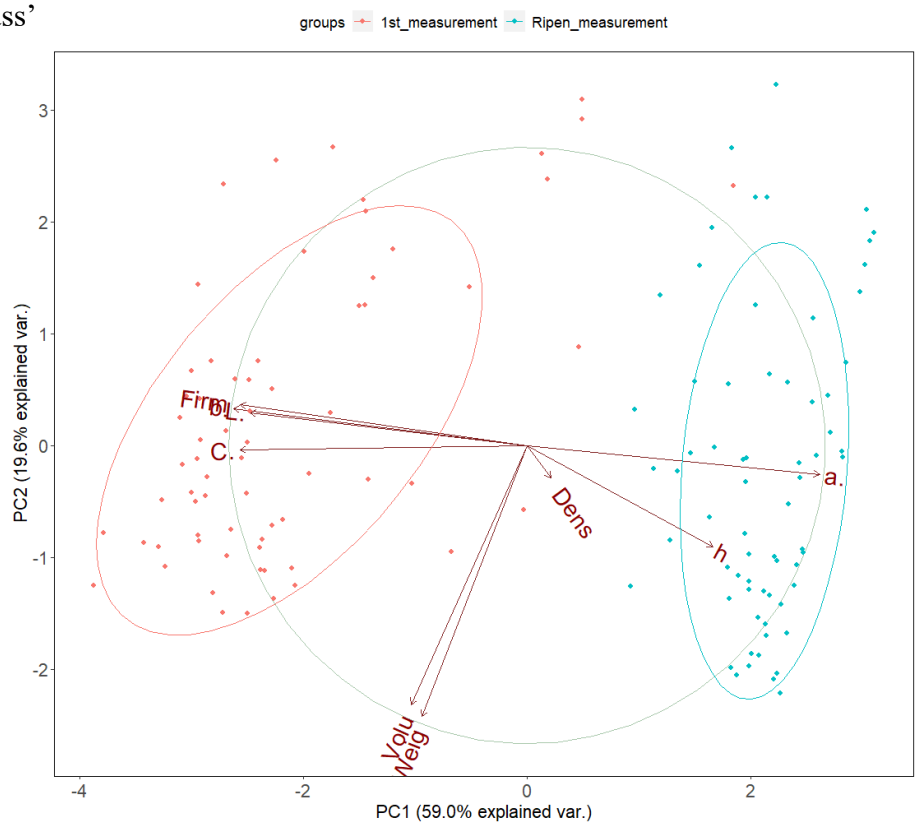

Fig. 16. The plots of principal component analysis showing strength of relevance of each parameter to ripening in (A) ‘Red Fairy’, (B) ‘Choquette’, and (C) ‘Hass’. The variables are represented as follows; weight as Weig., volume as Volu., L* value as L., a* value as a., b* value as b., C* value as C., h value as h, firmness as Firm., and density as Dens.

doi:10.6342/NTU202302656

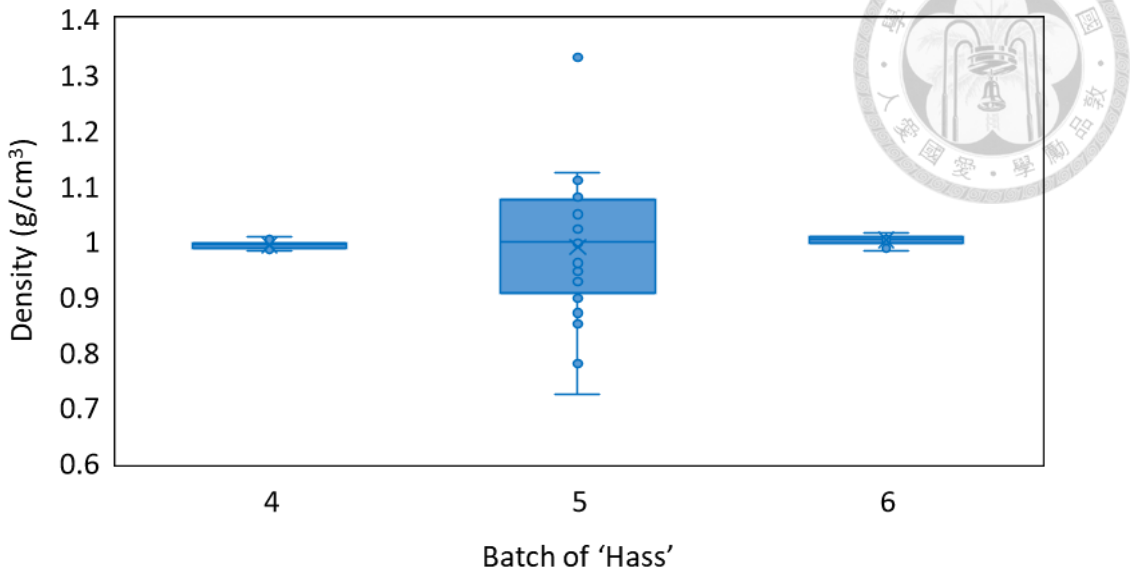

Fig. 17. Density range of 'Hass' fruits on Day 1. Fruit from batch 5 exhibited quite a wide range of density.

doi:10.6342/NTU202302656

A. ‘Red Fairy’

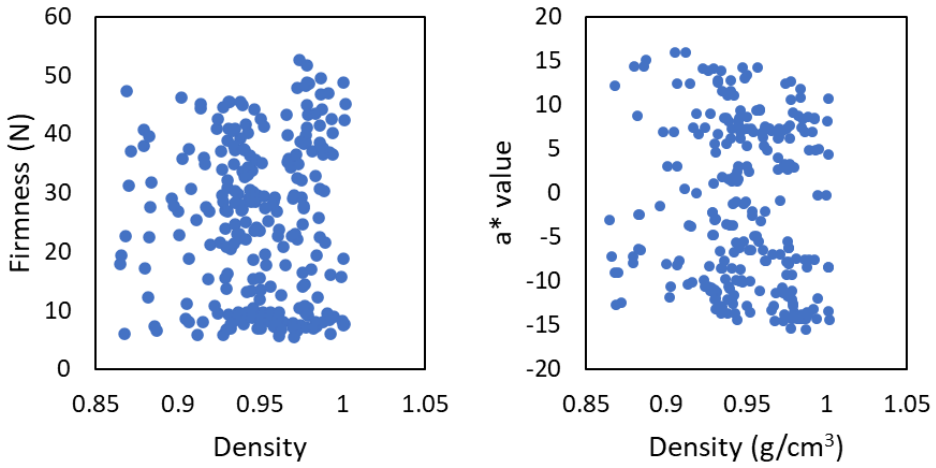

B. ‘Choquette’

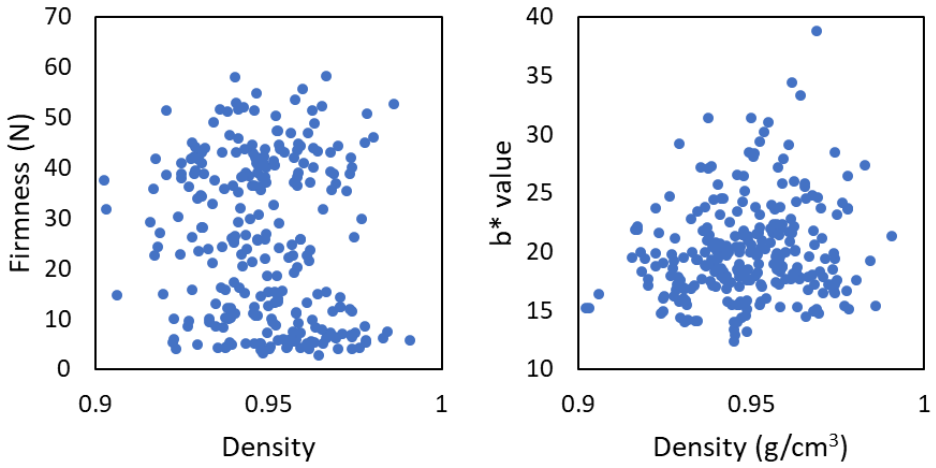

C. ‘Hass’

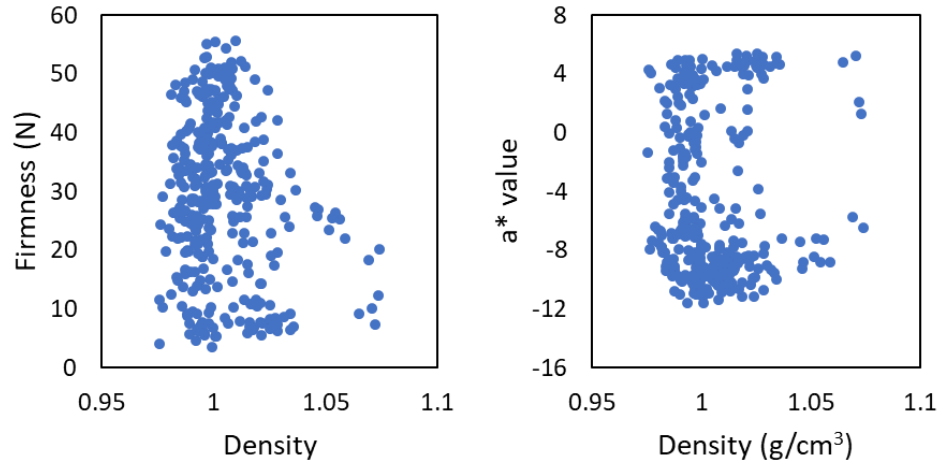

Fig. 18. Relationships between density and firmness or color value from all measurements in (A) ‘Red Fairy’, (B) ‘Choquette’, and (C) ‘Hass’.

doi:10.6342/NTU202302656

A. ‘Red Fairy’

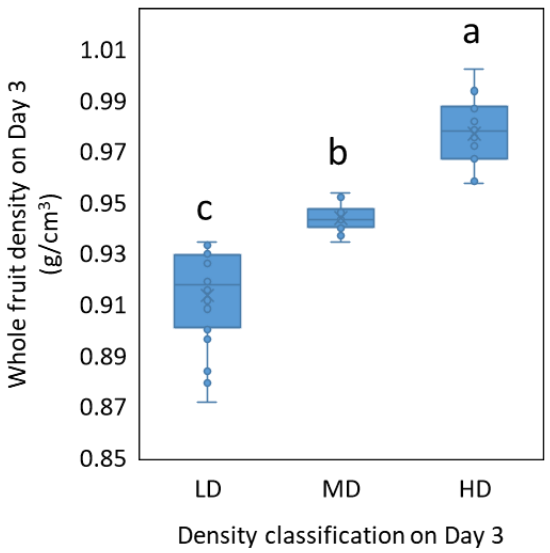

B. ‘Choquette’

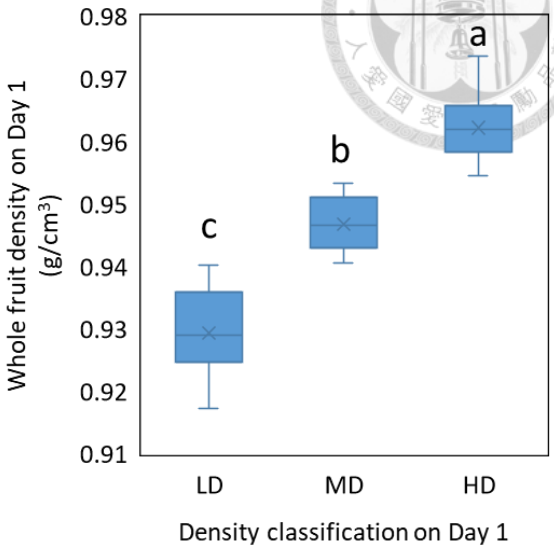

C. ‘Hass’

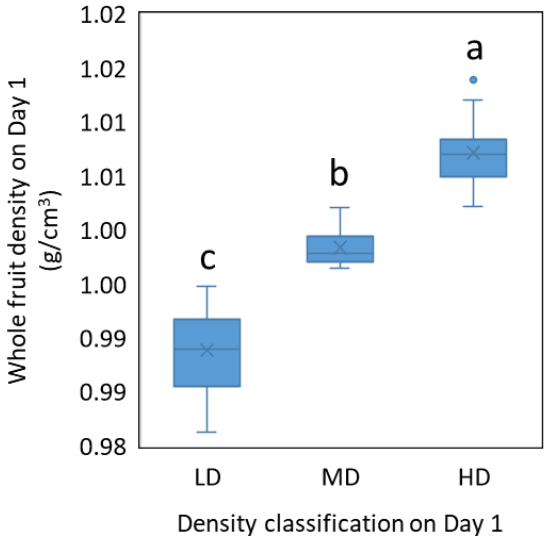

Fig. 19. Distribution of density among different density groups in (A) ‘Red Fairy’, (B) ‘Choquette’, and (C) ‘Hass’. Different letters indicate significant differences $p < 0.001$ by Steel-Dwass test.

doi:10.6342/NTU202302656

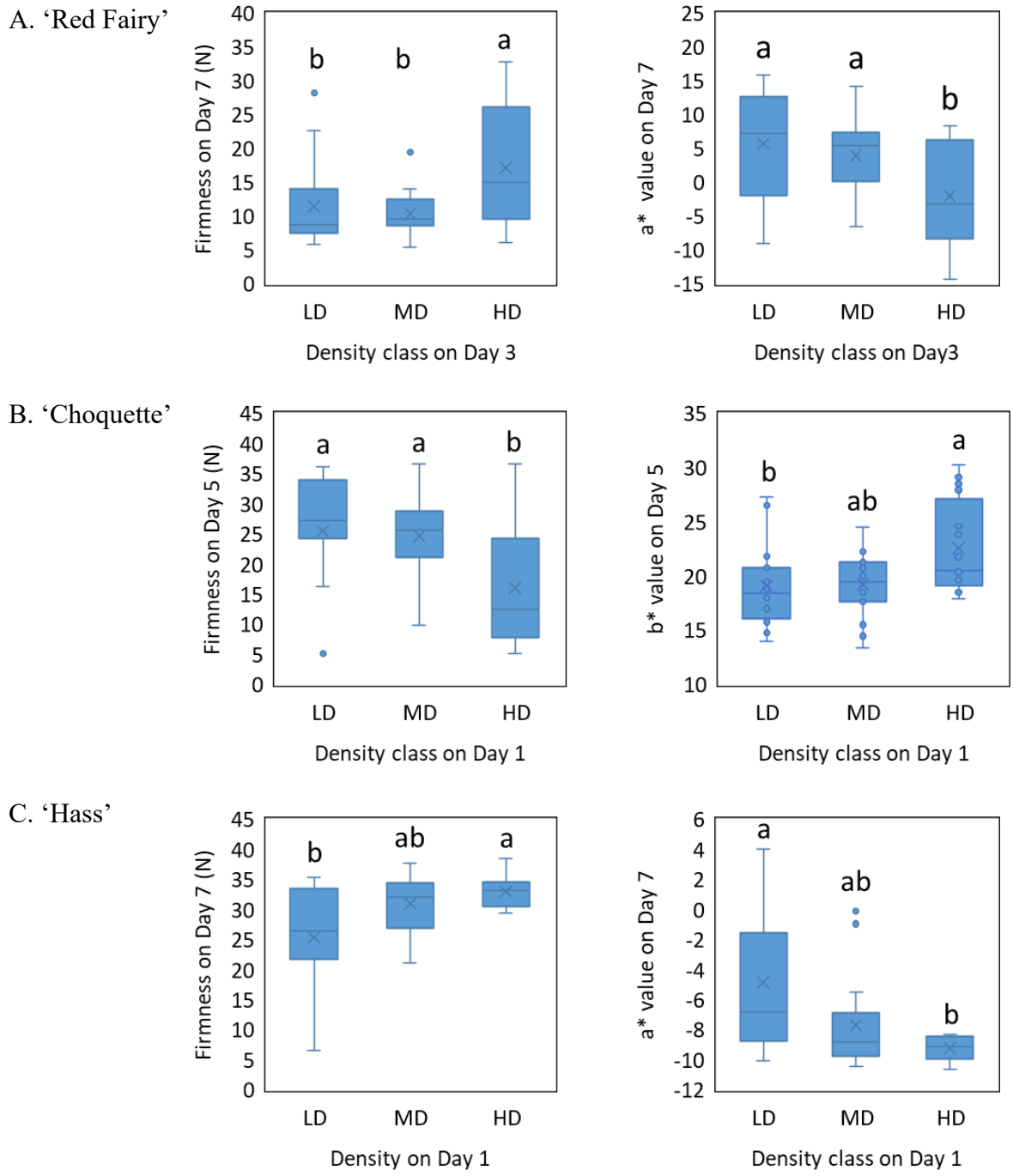

Fig. 20. Boxplots showing firmness and color differences among density groups in (A) ‘Red Fairy’, (B) ‘Choquette’, and (C) ‘Hass’. Firmness and color values were those of the earliest fruit reaching ripening. Different letters indicate significant differences at $p < 0.05$ by Steel-Dwass test.

doi:10.6342/NTU202302656

A. ‘Red Fairy’

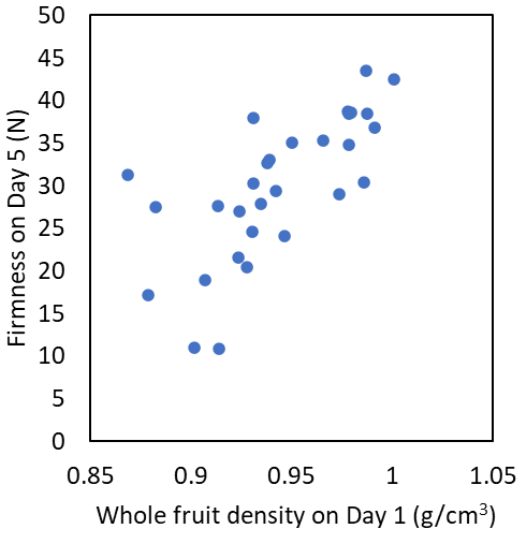

B. ‘Choquette’

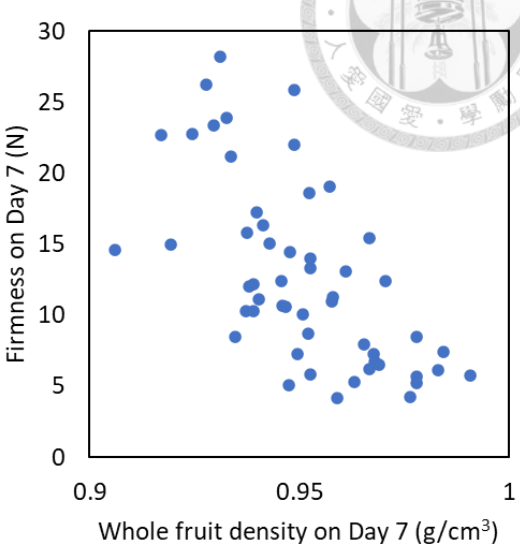

C. ‘Hass’

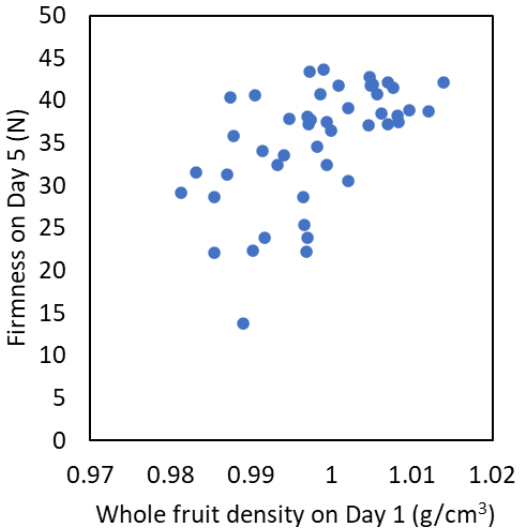

Fig. 21. Relationships between whole fruit density and firmness where the maximum R-squared was observed in the regression analysis

doi:10.6342/NTU202302656

A. ‘Red Fairy’

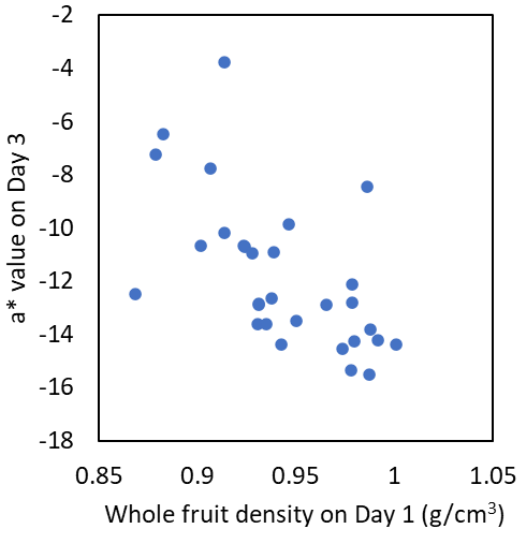

B. ‘Choquette’

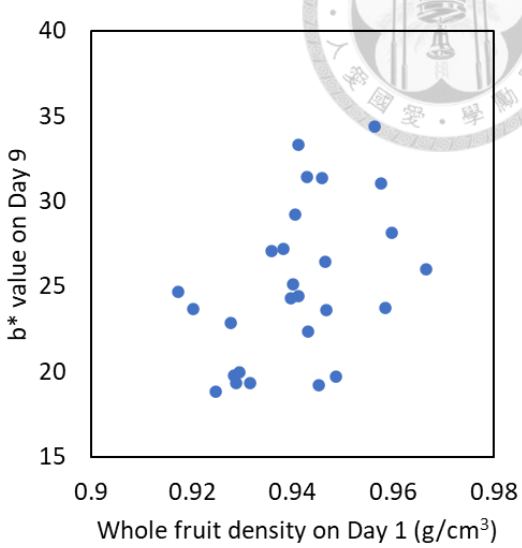

C. ‘Hass’

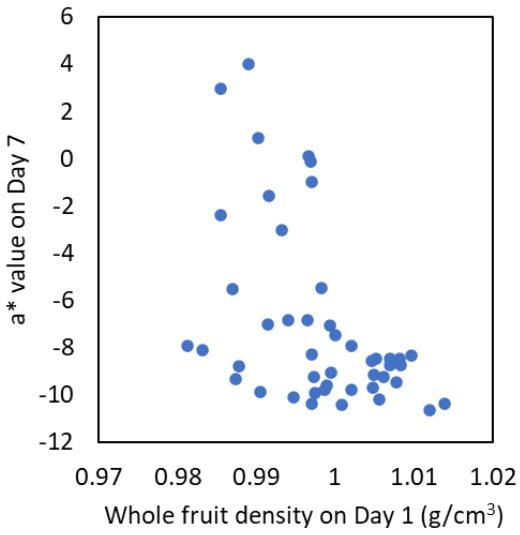

Fig. 22. Relationships between whole fruit density and color values where the maximum R-squared was observed in the regression analysis

doi:10.6342/NTU202302656

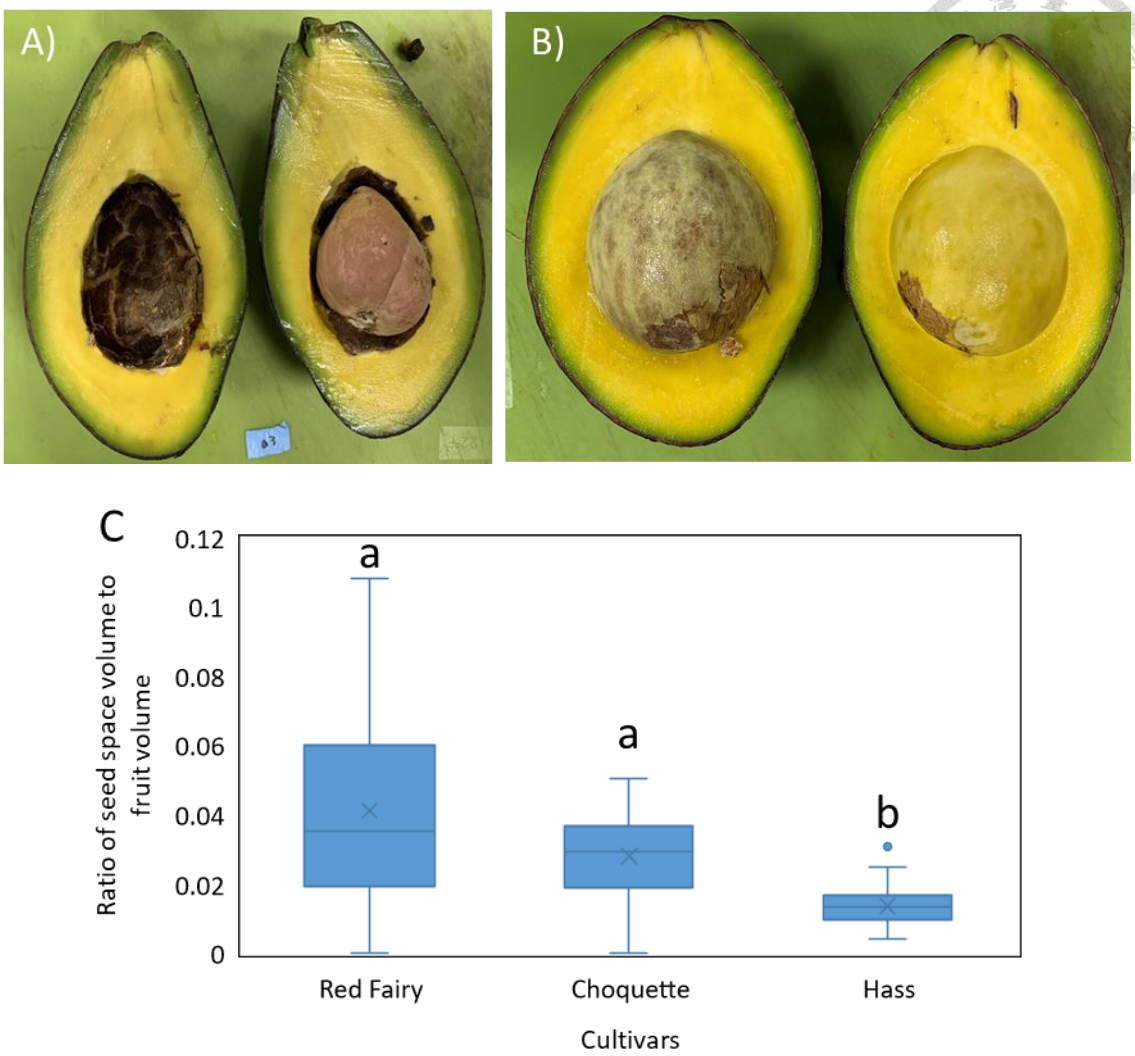

Fig. 23. Cross sections of avocado fruit and the magnitude of seed space in fruit. (A) 'Red Fairy' fruits with relatively big seed space and (B) 'Red Fairy' fruits with almost no seed space. (C) significance of seed space in 3 cultivars. Different letters indicate the significant difference at $p < 0.001$ by Steel-Dwass test. Seed space represents the space between seed and flesh, with its volume calculated by subtracting seed volume from seed cavity volume.

doi:10.6342/NTU202302656

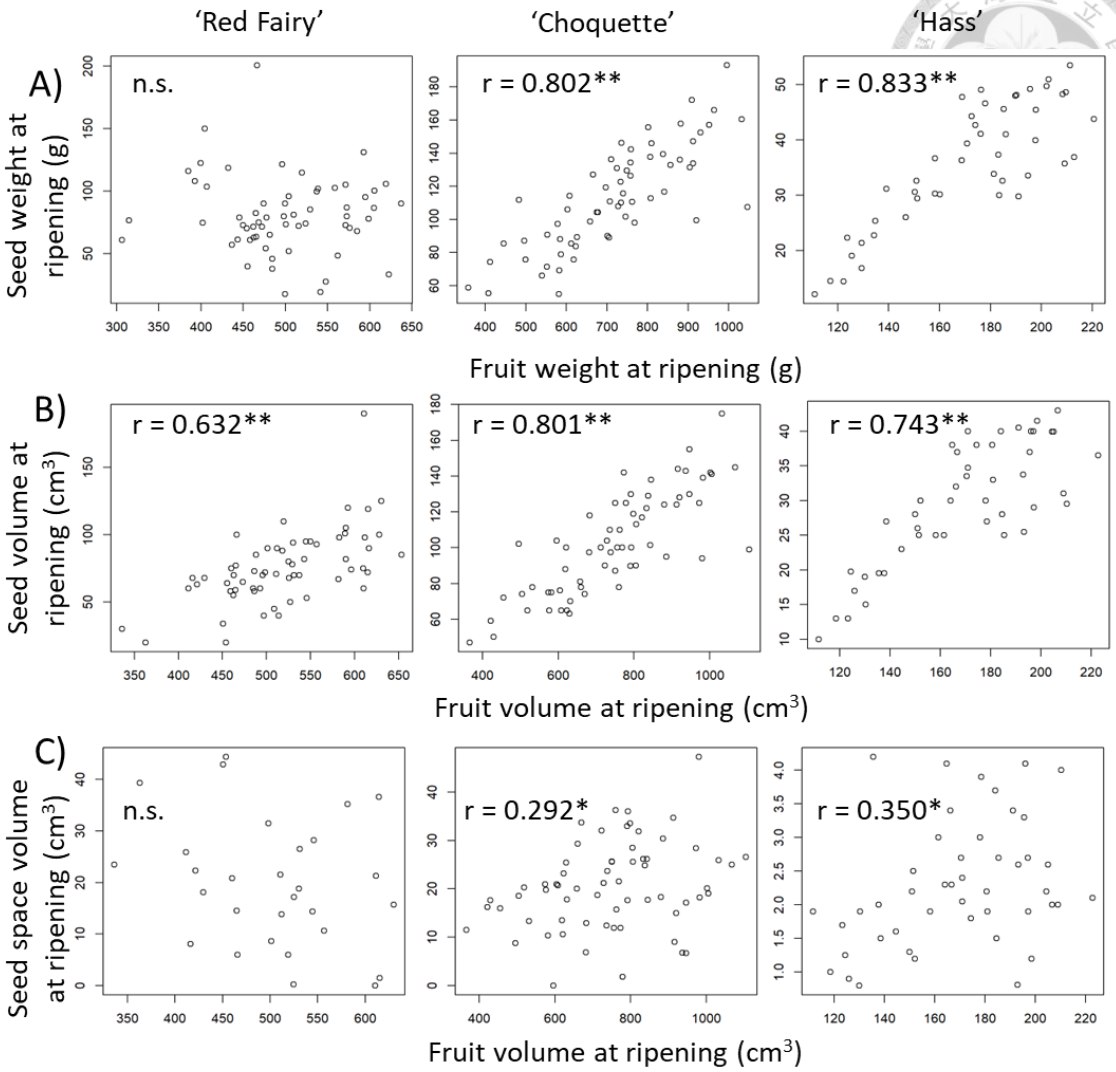

Fig. 24. Scatter plots showing the relationships between seed size or seed space, and fruit size. Relationships between (A) seed weight and fruit weight at ripening, (B) seed volume and fruit volume at ripening, and (C) seed space volume and fruit volume at ripening. Asterisks indicate the significance at $p < 0.05$ (*) and $p < 0.01$ (**), and n.s. represents that there was no significant correlation.

doi:10.6342/NTU202302656

A. ‘Red Fairy’

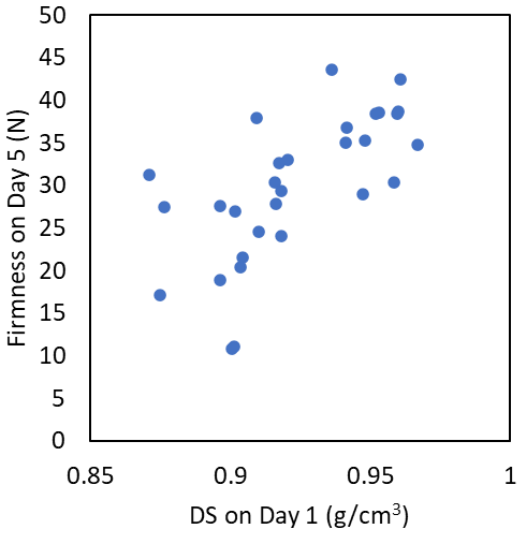

B. ‘Choquette’

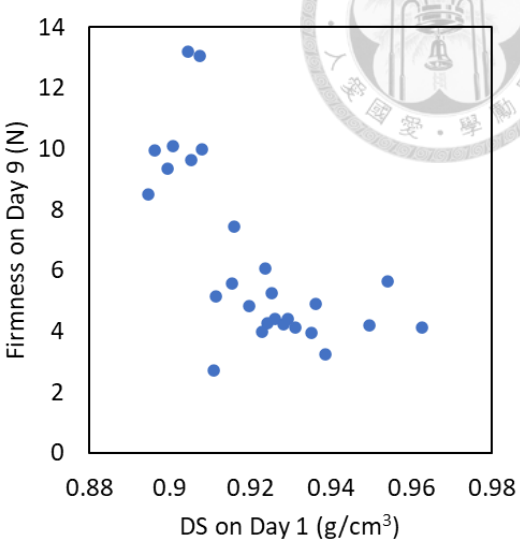

C. ‘Hass’

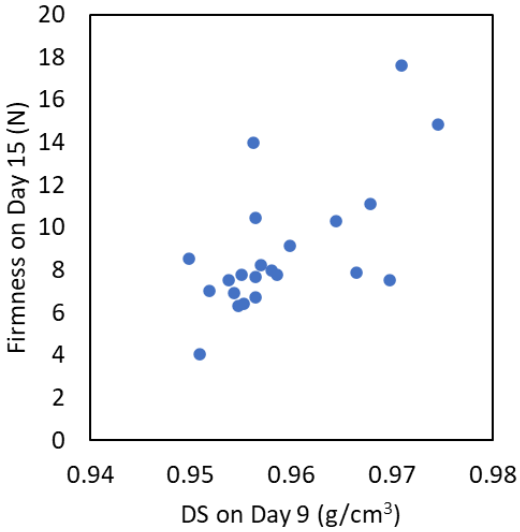

Fig. 25. Relationships between density subtracting seed size (DS) and firmness where the maximum R-squared was observed in the regression analysis. DS on day 9 was calculated by the formula of (fruit weight on day 9 – seed weight at ripening) / (fruit volume on day 9 – seed volume at ripening).

doi:10.6342/NTU202302656

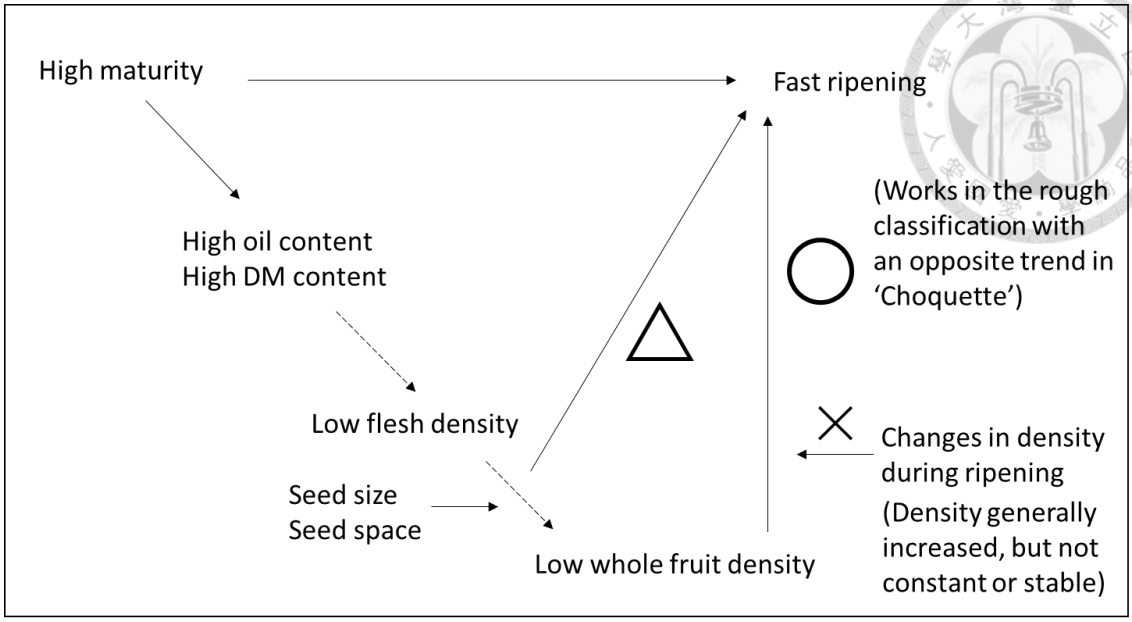

Fig. 26. Summary of the relationships among maturity, ripening, and density found in this study.

doi:10.6342/NTU202302656

A. ‘Choquette’

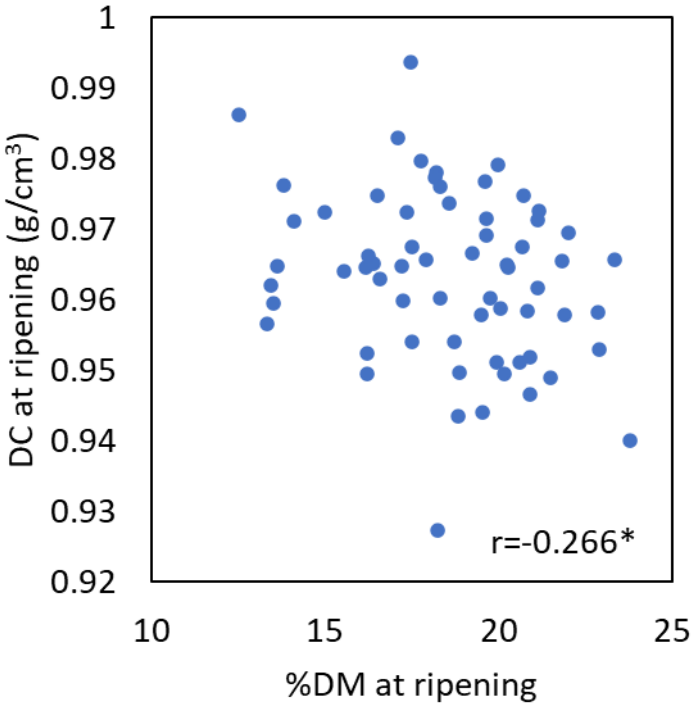

B. ‘Hass’

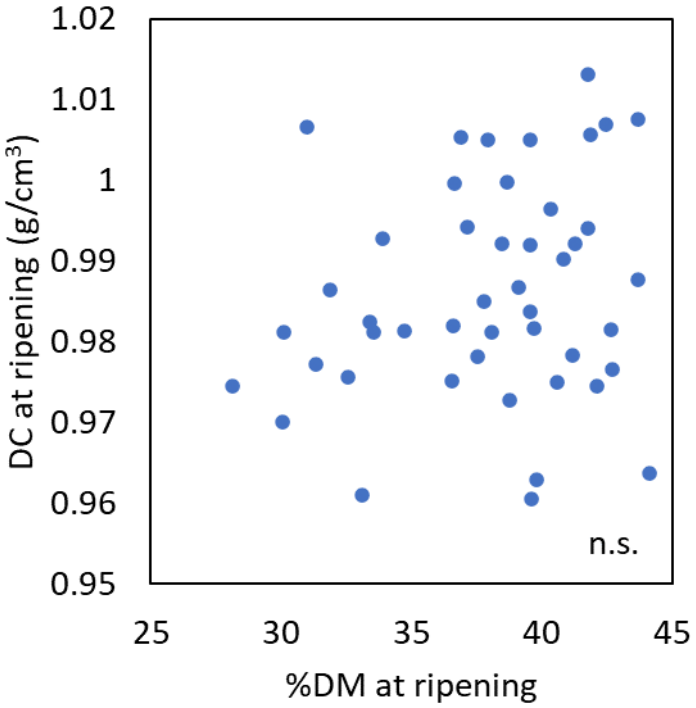

Fig. 27. Relationships between dry matter (DM) content and density subtracting seed size and space (DC) at ripening in (A) ‘Choquette’ and (B) ‘Hass’

doi:10.6342/NTU202302656

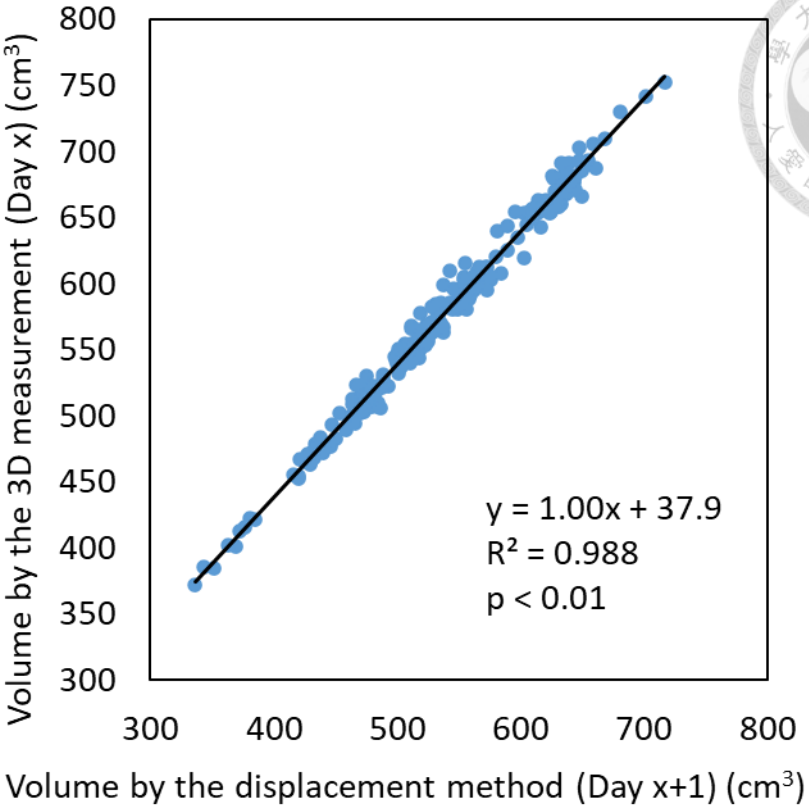

Fig. 28. A plot of the volume of 'Red Fairy' fruits measured by the displacement method and volume measured by the 3D reconstruction method. Since volume measurements in 2 different ways were not done on the same day, it was represented as Day x in the 3D reconstruction method and Day x+1 in the displacement method. X represents even numbers from 2 to 1 day before the ripening.

doi:10.6342/NTU202302656

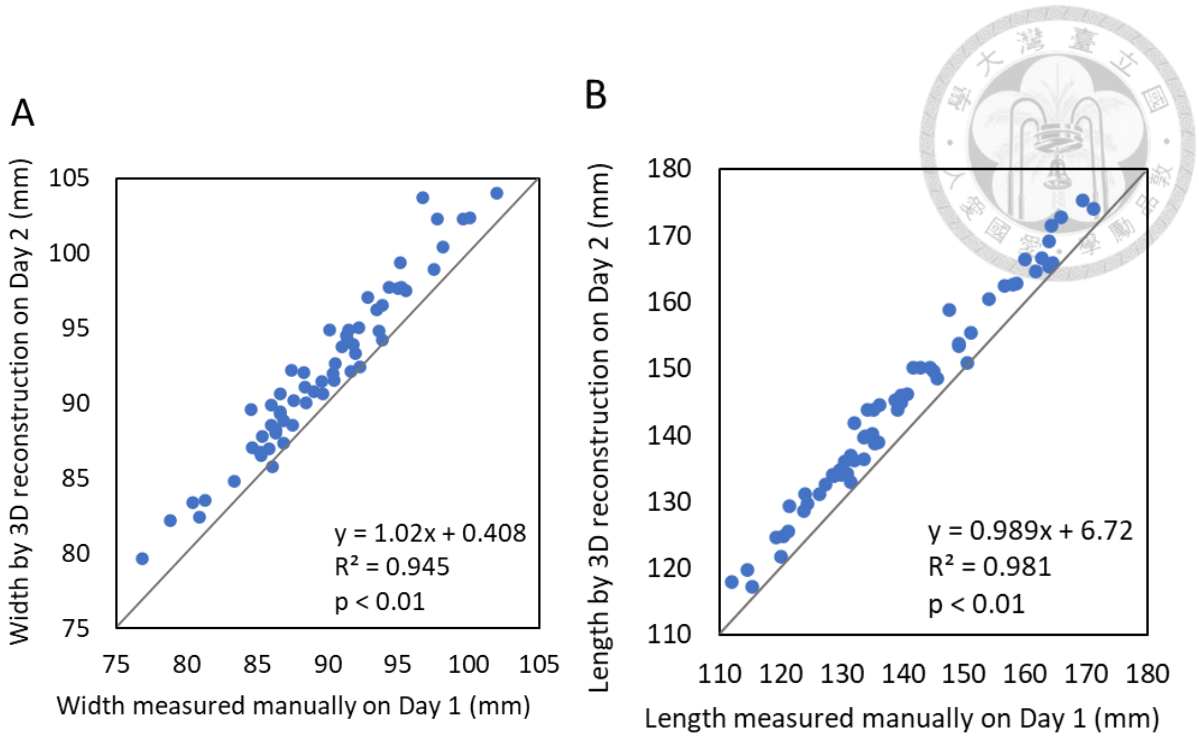

Fig. 29. Plots of the (A) fruit width and (B) fruit length of 'Red Fairy' fruits measured by the displacement method and volume measured by the 3D reconstruction method. Since the first 3D reconstruction models were developed on day 2, it was compared with the fruit width or length manually measured on Day 1. Black lines represent 1:1 relationship.

doi:10.6342/NTU202302656

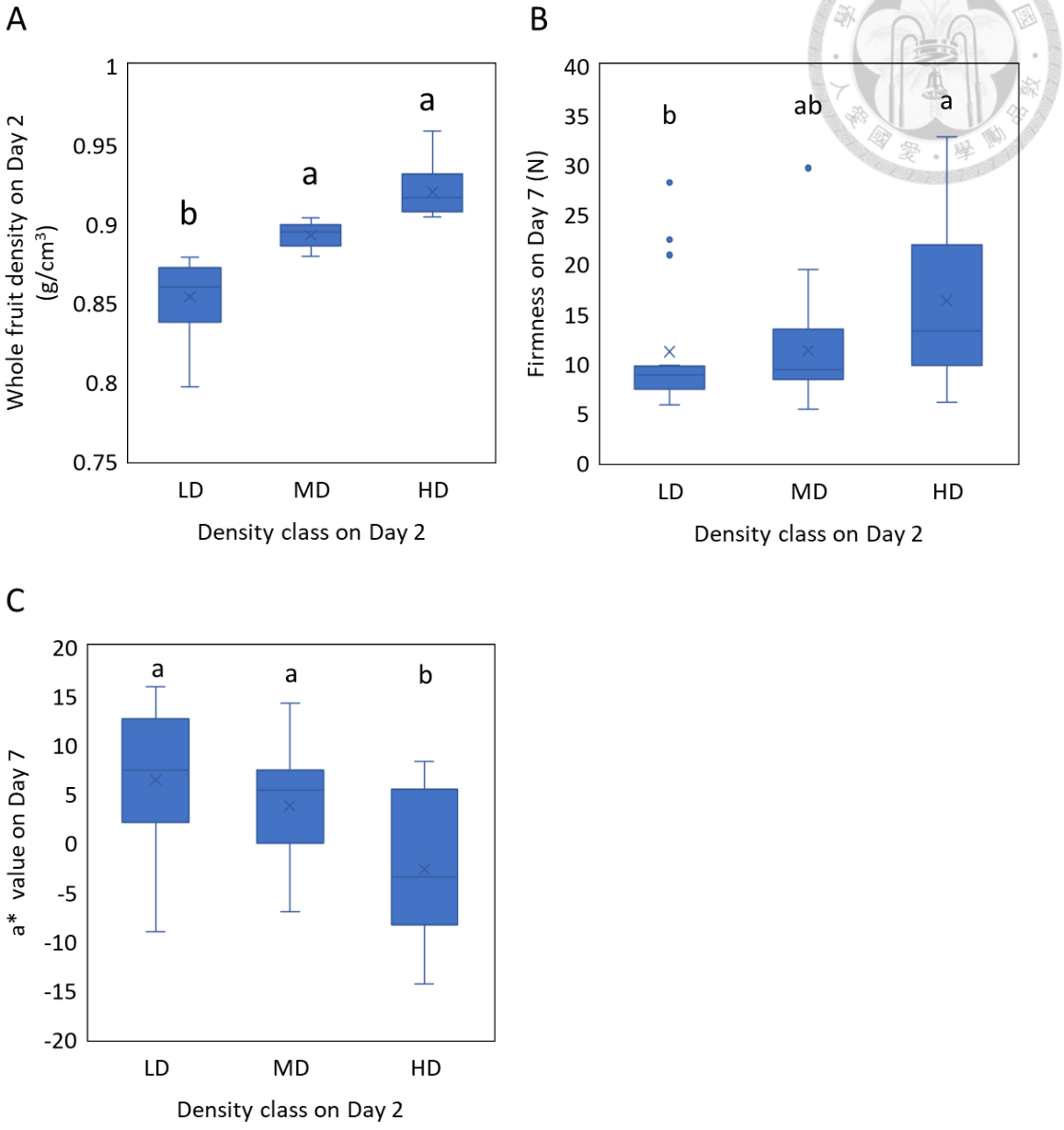

Fig. 30. Boxplots showing density, firmness, and color differences among density groups based on the 3D reconstruction method. Differences in (A) whole fruit density on Day 2 (B) firmness on Day 7 and (C) a* value on Day 7 among density groups in 'Red Fairy'. Different letters indicate significant differences $p < 0.05$ by Steel-Dwass test.

doi:10.6342/NTU202302656